X-723-75-171
PREPRINT

SPACEBORNE CO_2 LASER COMMUNICATIONS SYSTEMS

JOHN H. McELROY
NELSON McAVOY
EDWARD H. JOHNSON
FRANK E. GOODWIN
B. J. PEYTON

JULY 1975

GSFC
GODDARD SPACE FLIGHT CENTER
GREENBELT, MARYLAND

Submitted for Presentation as an Invited Paper at the IEEE Electronics and Aerospace Systems Conference (EASCON), Sept. 29 - Oct. 1, 1975, Washington, D. C.

SPACEBORNE CO_2 LASER COMMUNICATIONS SYSTEMS

John H. McElroy
Nelson McAvoy
Edward H. Johnson
NASA/Goddard Space Flight Center

Frank E. Goodwin
Hughes Aircraft Company

B. J. Peyton
AIL, A Division of Cutler-Hammer

ABSTRACT

Projections of the growth of earth-sensing systems for the latter half of the 1980's show a data transmission requirement of 300 Mbps and above. Mission constraints and objectives lead to the conclusion that the most efficient technique to return the data from the sensing satellite to a ground station is through a geosynchronous data relay satellite. Of the two links that are involved (sensing satellite to relay satellite and relay satellite to ground), a laser system is most attractive for the space-to-space link. During 1975 a major step toward the development of CO_2 laser systems for space-to-space applications is being completed. This step is the completion of a 300 Mbps data relay receiver and its modification into a transceiver. The technology and state-of-the-art of such systems are described in detail in this paper.

CONTENTS

ILLUSTRATIONS

ILLUSTRATIONS (Continued)

TABLES

SPACEBORNE CO_2 LASER COMMUNICATIONS SYSTEMS

INTRODUCTION

The year 1975 marks the end of a five year effort to develop the technology for carbon dioxide laser intersatellite communication systems. This effort, directed by NASA's Goddard Space Flight Center, was conducted by a joint government-industry-university team with participants from Hughes Aircraft Company, Airborne Instruments Laboratory (AIL), S.A.T., Arthur D. Little, Inc., GTE Sylvania, the Technical University of Vienna (Austria), the University of Maryland, and the technical staff of Goddard's Laser Technology Branch. The program included component, subsystem, and system development and is culminating in the development of an engineering model transceiver capable of transmitting and receiving data at a rate of 300 Mbps. The receive channel is designed to accept Doppler shifts of ±700 MHz.

In the succeeding sections of this paper we will review the motivation for the development program, outline the fundamentals of CO_2 space communication systems, and discuss the present state-of-the-art.

MOTIVATION

The historic trend in communications has been a movement toward higher and higher frequencies, although that trend has not been without its abrupt leaps as one spectral region has yielded to application while another has not. The development program we describe here is an integral part of the trend toward higher frequencies. It was motivated by the same factors which have always influenced such trends, namely higher antenna gain for a given aperture and greater spectrum availability. In the case of carbon dioxide laser communication systems operating in the ten micrometer portion of the spectrum, these factors were coupled with the availability of an efficient source and the knowledge that the mechanical tolerances and antenna pointing requirements were within the capabilities of modern optical systems. It was on these fundamentals that the program was based. It was then necessary to structure a program which would create the system based on the CO_2 laser and, in the process, to fill obvious gaps in wideband modulation, mixer performance, laser lifetime, optical analysis for laser heterodyne systems, Doppler tracking techniques, and other areas. The development program is depicted in Figure 1.

While the above provides a plausible reason for conducting a research program, the establishment of an extensive development program also requires that the technology have pertinence to a projected organizational need. The need recognized

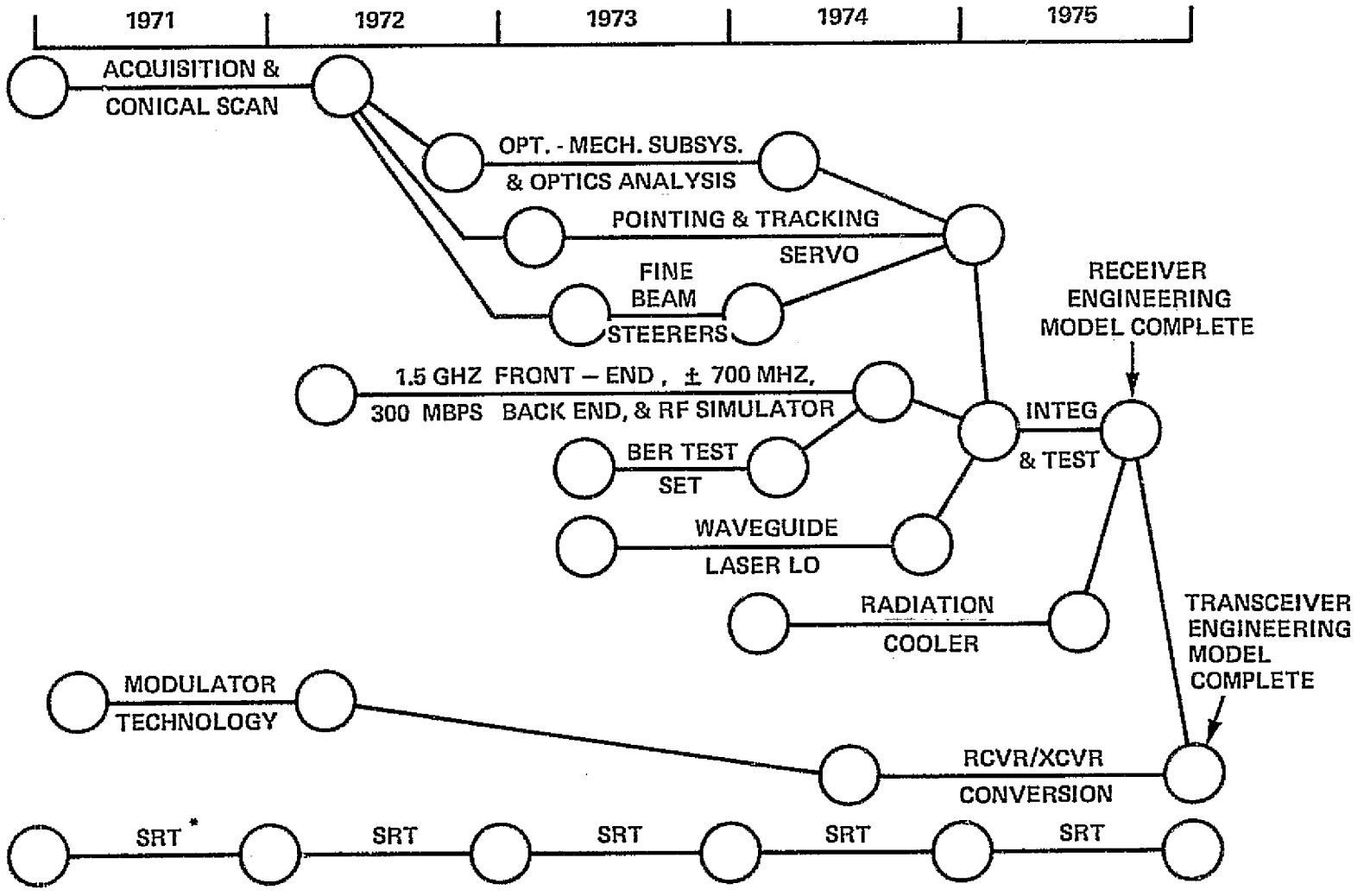

*SRT - Supporting Research and Technology

Figure 1. Development Plan for CO_2 Laser Engineering Model Transceiver

within NASA was the evolutionary growth of Earth sensing requirements which has been most vividly demonstrated by the Landsat (formerly the Earth Resources Technology Satellite) in the 1970's and which is projected to increase through the 1980's. The data rate resulting from a given sensing requirement is controlled by the linear dimension of the smallest resolvable object on the ground, the swath width observed by the sensor, the ground velocity of the satellite, and the number of bands in which the scene is observed. For example, a scene observed with 10 meter resolution, a swath width of 185 km, observed from a typical altitude (and hence, ground velocity), and simultaneously viewed in 10 spectral bands in the visible and near-infrared produces a 1 Gbps uncompressed data rate. Projections of the NASA Earth sensing data rate requirements for the late 1980's show processed rates in the range of 300 to 500 Mbps.[1] The collection of data at such rates is most readily accomplished by a network of geosynchronous relay satellites which provide for real-time read-out of data from multiple sensor spacecraft and "bent-pipe" relay to a ground station. Subsequent distribution of data to users would then be made via a domestic communications satellite as depicted in Figure 2. All intersatellite links are assumed to use laser systems, while all satellite-ground links use RF systems. The advantages to be gained from laser intersatellite links include compactness (as demonstrated in Figure 3(a) and 3(b) which depicts one of several competitive sensing satellite concepts), freedom from frequency allocation limits (which limit a K_u-band intersatellite link to about 300 Mbps), and freedom from interference due to terrestrial RFI. Figure 4 shows a concept for a laser-augmented Advanced Tracking and Data Relay Satellite (ATDRS). Two high data rate users can be accomodated simultaneously and the use of polarization diversity on the ATDRS-ground K_u-band link permits data rates up to 600 Mbps on that link. Transceivers on the sides of the ATDRS permit one ATDRS to communicate with another; this avoids the use of a ground station to relay data between two ATDRS's. Such a situation occurs when a sensing satellite on the opposite side of the Earth must return data to a central processing facility. Within the above context, we will now review the fundamentals of CO_2 laser space communication.

FUNDAMENTALS

Receiver Sensitivity

In common with other laser systems, CO_2 laser receivers operate in the quantum-limited regime and use heterodyne detection in common with RF systems. A general expression for receiver noise is[2]

$$\frac{P_N}{B} = \frac{hf}{\exp(hf/kT) - 1} + \frac{hf}{\eta} \qquad (1)$$

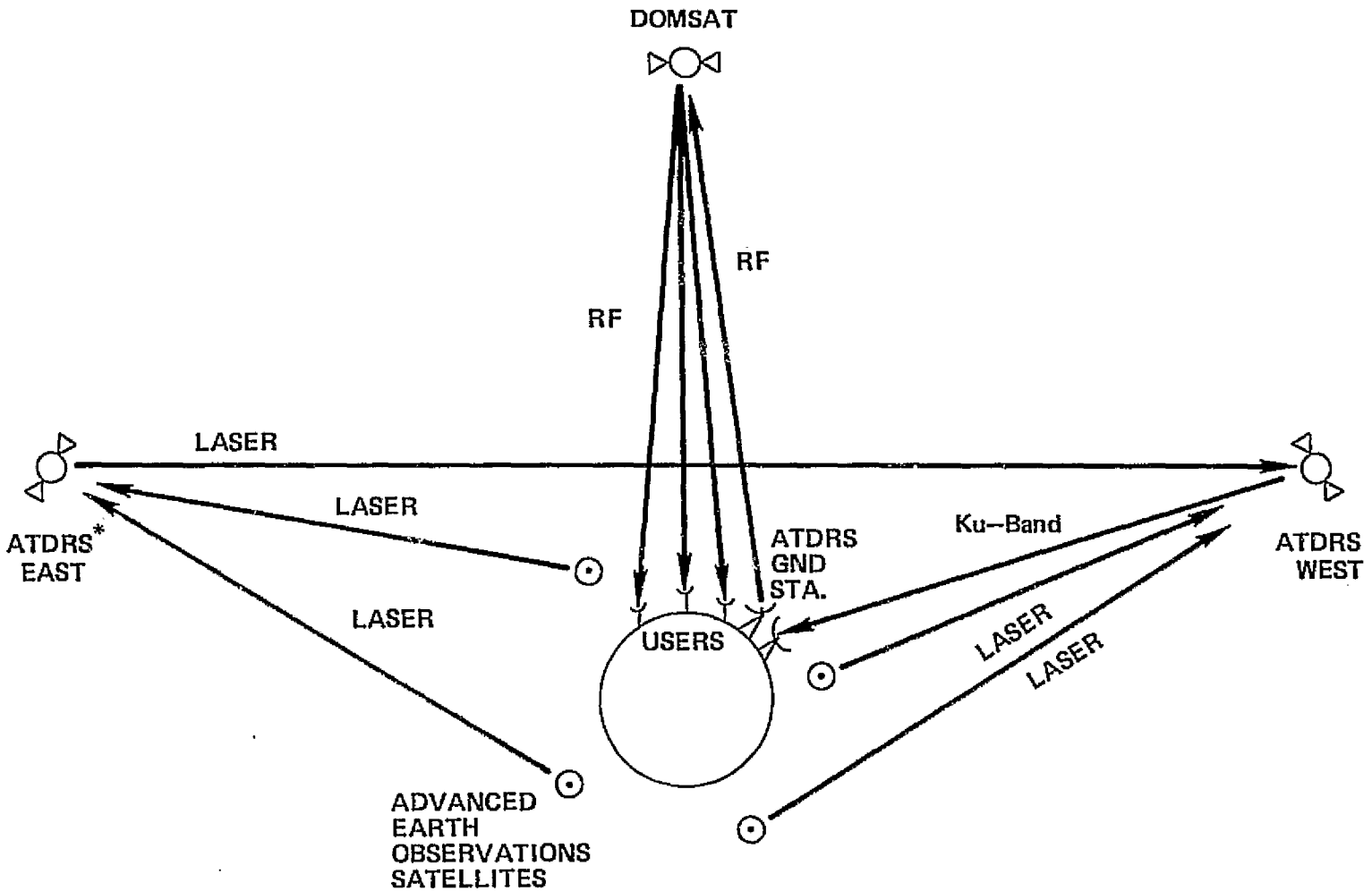

*ATDRS - Advanced Tracking and Data Relay Satellite

Figure 2. Earth-Sensing Satellite Relay System Concept for the Late 1980's

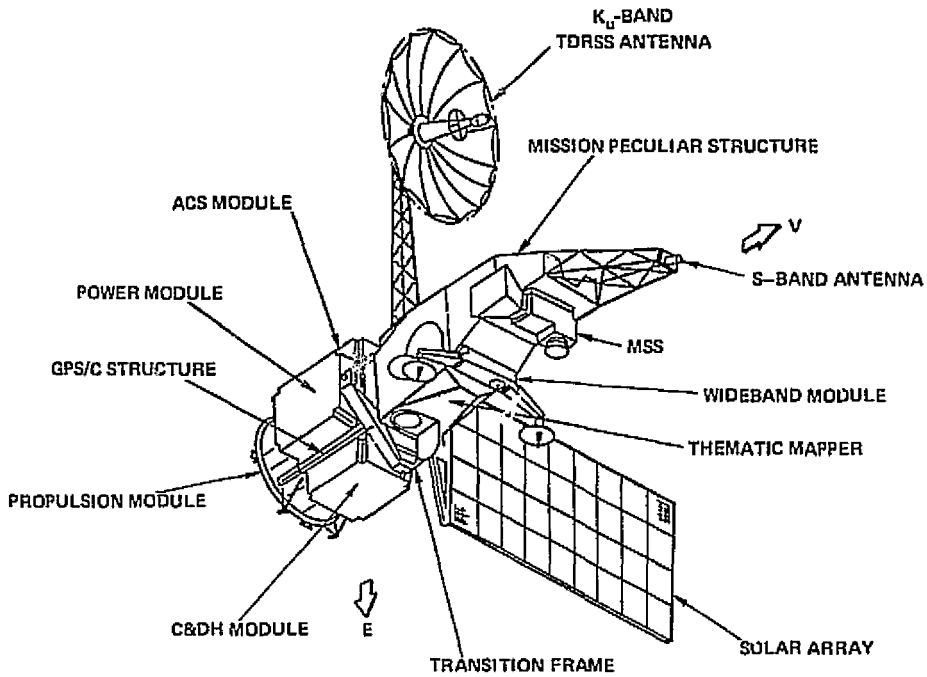

(a) Sensing Satellite Configuration Using K_u-Band System (up to 300 mbps).

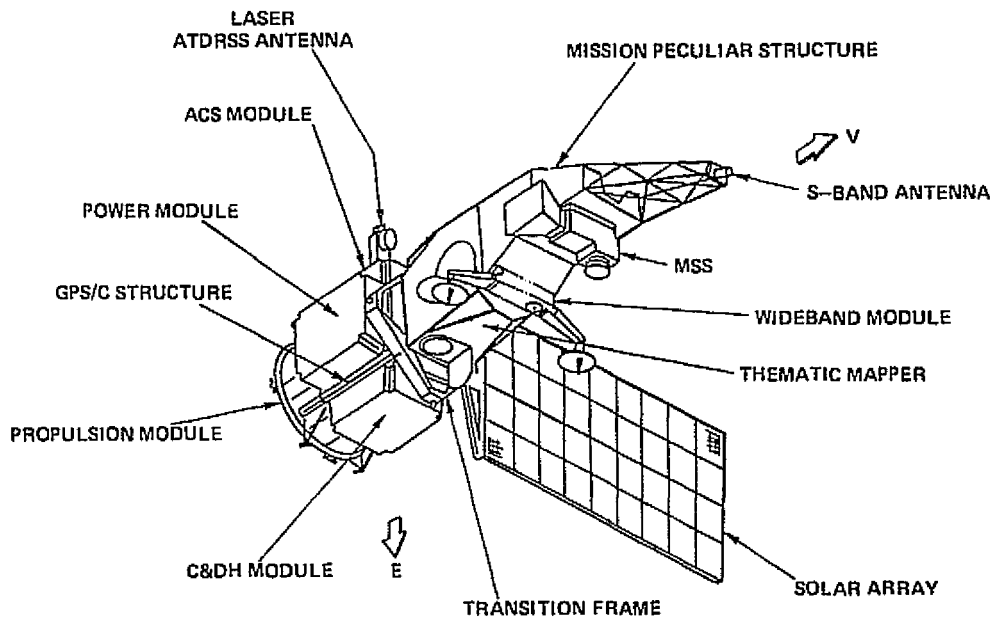

ATDRSS - Advanced Tracking and Data Relay Satellite System

(b) Sensing Satellite Configuration Using CO_2 Laser System (300–600 mbps Data Rate)

Figure 3. Earth-Sensing Satellite Configurations (One of Several Possible)

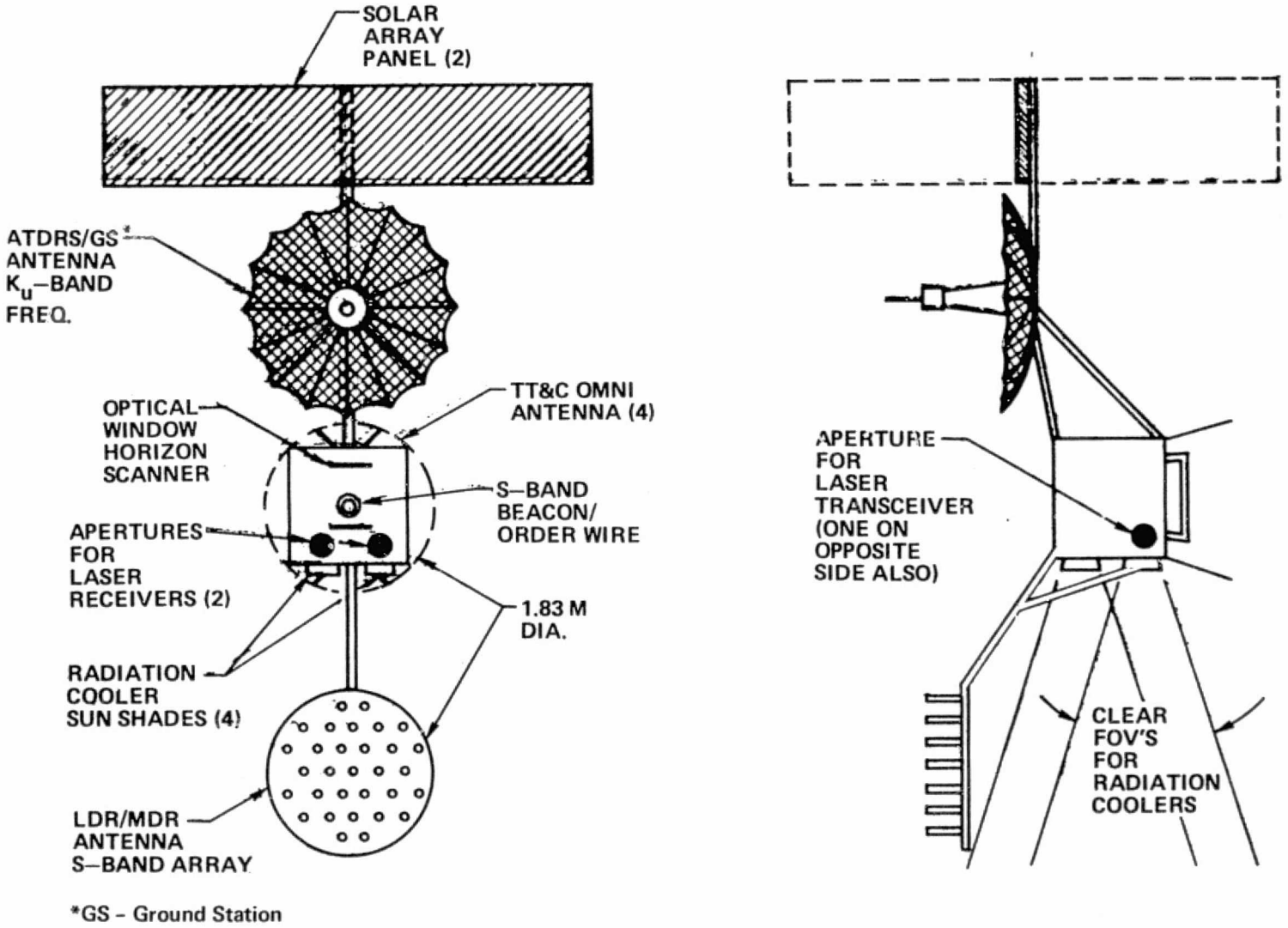

Figure 4. Laser-Augmented Advanced Tracking and Data Relay Satellite (ATDRS) Concept

where P_N is the noise power, B is the bandwidth, h is Planck's constant, T is the background black-body temperature, and η is the efficiency with which incoming photons are absorbed by the mixer. At RF frequencies, the first term dominates and Equation (1) becomes

$$\frac{P_N}{B} = kT \tag{2}$$

while at laser frequencies the second term dominates and we have

$$\frac{P_N}{B} = \frac{hf}{\eta} \tag{3}$$

Equation (1) is plotted in Figure 5; for a 290°K temperature background, the cross-over between the two occurs near 50 micrometers. By letting the quantum efficiency be an "effective" quantum efficiency which includes the actual quantum efficiency as well as other noise contributions—such as that due to the noise figure of the mixer preamplifier—we have a direct analogy to the microwave practice. In the case the "T" is similarly an "effective" noise temperature. As will be noted in the subsequent discussion of the state-of-the-art, a representative value of P_N/B for a ten-micrometer system is 10^{-19} W/Hz.

Antenna Gain

The optical systems, which can be called "telescopes" loosely, used in laser communication systems are entirely equivalent to the antennas used in microwave systems. They, therefore, obey the same antenna gain relationships as more conventional systems. The limiting gain of either an RF or an optical antenna is given by[3]

$$G = \frac{4\pi A}{\lambda^2} \tag{4}$$

where A is the antenna area (assumed to be circular) and λ is the wavelength. Klein, Degnan, and Cohen[4,5,6] have completed a detailed examination of optical antennas as a part of the development program shown in Figure 1. By noting that the beamwidth, θ, between half-power points is approximately λ/D (where D is the diameter of the antenna), Equation (4) can be rewritten in the useful form

$$G = (\pi/\theta)^2 \tag{5}$$

Probably the most striking feature of a laser communication system is the narrow antenna beamwidths and the corresponding high antenna gains. For example,

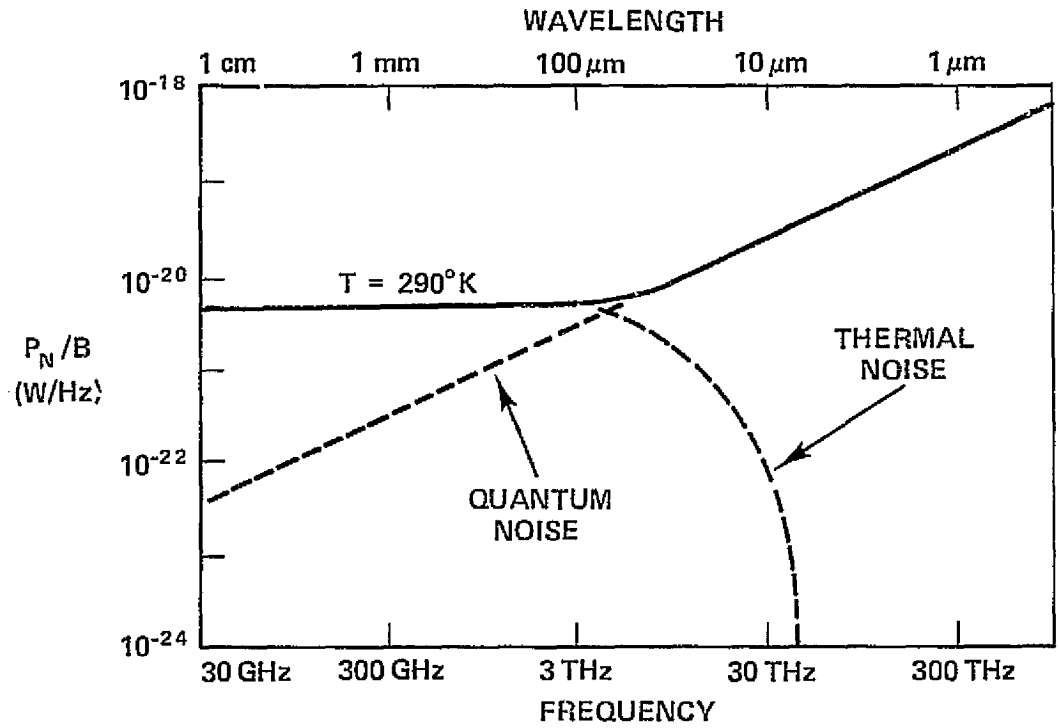

Figure 5. Receiver Noise Spectrum

a 25-cm (10-in.) diameter antenna produces a beamwidth of 40 microradians (8 seconds of arc) at ten micrometers; this corresponds to an antenna gain of 98 dB. Such values lead to the need for carefully designed acquisition and tracking systems—our next topic.

Acquisition and Tracking

The narrow beams associated with laser communications prohibit, in most practical space systems, the use of systems in which communication is established in one direction only. In all of the systems considered in this paper, the wideband transmitter requires illumination by a beacon source which is received by a beacon receiver at the transmitter. The beacon receiver establishes a reference direction which is used by the terminal to point the transmitter. This requirement necessitates that a transmitter on an Earth-sensing satellite in low-altitude orbit also have a beacon receiver. Similarly, a receiver on a geosynchronous relay satellite must also have a beacon transmitter. These requirements are depicted in Figure 6. We have summarized the steps required for acquisition in Table 1. The low-altitude sensing satellite is designated LAS in the table and the synchronous orbit relay satellite is designated SRS.

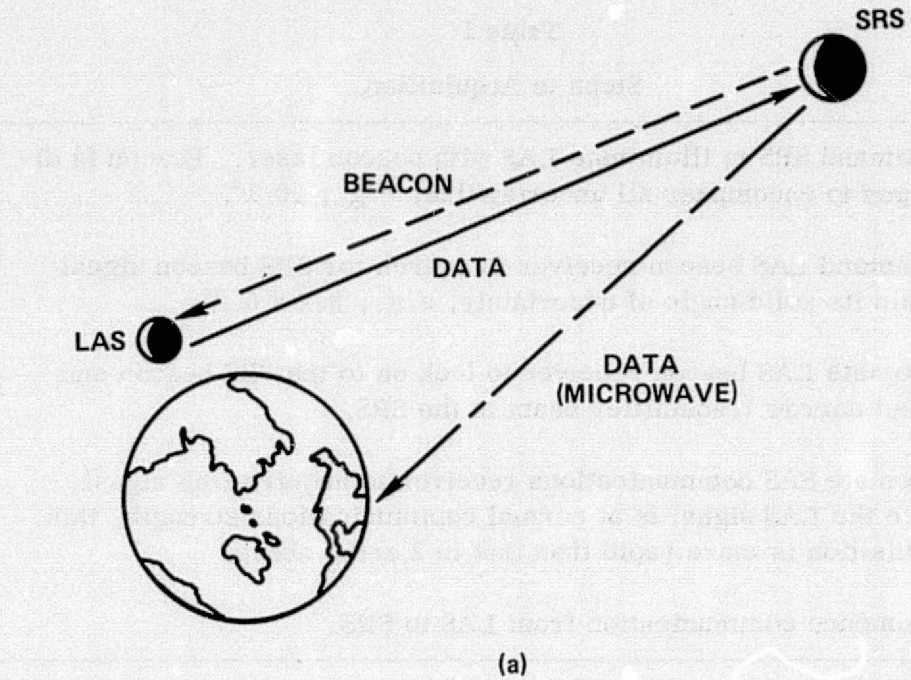

(a)

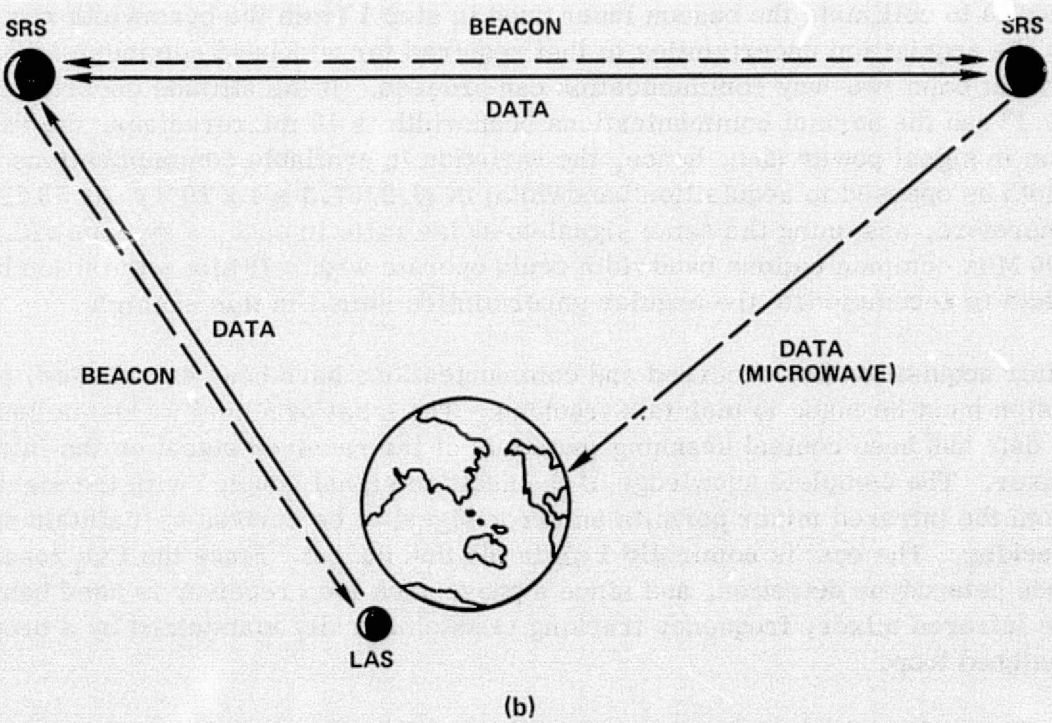

(b)

Figure 6. Data Relay Modes

Table 1

Steps in Acquisition

1. Command SRS to illuminate LAS with beacon laser. Beacon is diverged to encompass all uncertainties, e.g., ±0.1°.

2. Command LAS beacon receiver to search for SRS beacon signal within its solid angle of uncertainty, e.g., 0.2 x 0.2°.

3. Automate LAS beacon receiver to lock on to the SRS beacon and direct narrow transmitter beam at the SRS.

4. Automate SRS communications receiver to acquire LAS signal. Since the LAS signal is at normal communications strength, this acquisition is more rapid than that in 2 and 3 above.

5. Commence communication from LAS to SRS.

In the event that it is necessary to establish two-way wideband communications, as in the case of a link between two SRS's, a further step is necessary. This step is to collimate the beacon laser used in step 1 from the beamwidth required by the acquisition uncertainties to that required for wideband communication. At that point two-way communication can proceed. If the attitude uncertainty is ±0.1° and the normal communications beamwidth is 40 microradians, the variation in signal power (and, hence, the variation in available communications bandwidth as opposed to acquisition bandwidth) is $(0.2/57.3 \times 4 \times 10^{-5})^2$ or 39 dB. Therefore, assuming the same signal-to-noise ratio in each, a system with a 600 MHz communications bandwidth could operate with a 79 kHz acquisition bandwidth to accommodate the angular uncertainties stated in this example.

After acquisition has occurred and communications have been established, provision must be made to maintain tracking. The most practical technique found to date has been conical scanning (nutation) of the received signal on the infrared mixer. The complete knowledge of the nutation signal coupled with the signal from the infrared mixer permits an error signal to be derived to maintain spatial tracking. The cost is nominally 1 dB in the link budget. Since the CO_2 laser uses heterodyne detection, and since a phase-lock loop receiver is used behind the infrared mixer, frequency tracking is automatically maintained by a properly designed loop.

Early results on the acquisition technique and the conical scanning system have been published,[7] while more recent results are available in contract reports.[8,9]

It is probably evident by this point that CO_2 laser communications systems are closely related to their RF counterparts. Another area of evident common ground is modulation techniques; here, however, a few pitfalls await. We will explore them now.

Modulation Techniques

CO_2 lasers can be amplitude, phase, or frequency modulated; the latter two, however, are limited because of either excessive power consumption or physical restrictions of the laser itself. This led to the selection of a modulation technique known as "coupling modulation." This technique is analogous, although not identical, to double sideband suppressed carrier modulation.[10,11,12,13] In coupling modulation an electro-optic crystal located in a plane-polarized laser produces a component orthogonal to that polarization which is then coupled out of the cavity by a polarization selective device. This occurs whenever a voltage is applied to the electro-optic crystal. The amount of power coupled from the cavity is related to the applied voltage, the amount of circulating power in the laser cavity (resonator), and other parameters. In practice the other parameters are adjusted to their best possible values and the only remaining degrees of freedom are the modulator voltage and the circulating power. This leads to one of the distinctive characteristics of CO_2 laser systems in comparison to RF systems. In a laser system the transmitter power burden is dependent upon the sum of two large components, the modulator power and the laser's circulating power. A sophisticated trade-off must be made to obtain the minimum transmitter power burden.[14,15] A common error is to treat the laser system like an RF system and assume that the laser efficiency dominates the power burden. With this important exception noted we are now free to return to the area of close similarities—namely link analysis.

Link Analysis

Table 2 gives the link analysis for the relay of 300 Mbps data from a low-altitude satellite to a synchronous relay satellite; the same format is used as is customarily used in RF systems. Since the CO_2 laser system is limited by additive white Gaussian noise (AWGN), the basic relationships between signal-to-noise ratio and probability of error apply which are available in such standard references as Wozencraft and Jacobs[16] and Van Trees.[17] The 95 dB transmitting antenna gain corresponds to the use of a 20.3 cm (8 in.) effective diameter antenna and the 97 dB receiving antenna corresponds to a 25.4 cm (10 in.) effective diameter antenna. Two comments are in order here: (1) The optical antenna systems discussed in this paper do not obey transmit/receive reciprocity. Because the transmitting antenna aperture is illuminated by a Gaussian beam (produced by the fundamental laser transmitter mode) and the receiving antenna aperture is illuminated by a plane wave, the gain of the same aperture

Table 2

Link Analysis: Low-Altitude Satellite to Synchronous Satellite
(300 Mb/sec)

Parameter	Value (dB)
Transmitted Power	0
Transmitting Antenna Gain	95
Transmitting Losses	-2
Pointing and Conical Scan Losses	-1
Space Loss (Maximum Range)	-274
Receiving Antenna Gain	97
Receiver Losses	-3
N_o	-190
B	-85
CNR	17
Required CNR	13
Margin	4

is typically 2dB less in reception. (2) The beamwidth (between half-power points) for the 20.3 cm aperture is 52.2 microradians, which is quite close to the typical maximum "point-ahead" angle in the LAS-SRS link.[18] The point-ahead angle is the result of the transverse velocity component between the two satellites and merely means that, although the beacon receiver at the transmitter is locked on to the beacon signal from the SRS, that signal is originating from a point where the SRS was a period of time before (the time-of-flight between the two satellites). It also means that the transmit beam must be displaced from the receive axis by an amount which compensates for twice the time of flight.

Table 3 gives a link analysis for a 600 Mbps SRS-SRS system. The 97 dB transmitting and 99 dB receiving antenna gains correspond to the use of 30.5 cm (12 in.) effective diameter antennas. The beamwidth of these antennas is nominally 34.8 microradians and the point-ahead angle for the link averages 20 microradians.

With the above remarks on fundamentals as our context, we will now examine the state-of-the-art in the various components, subsystems, and systems for spaceborne CO_2 laser communication systems.

Table 3

Link Analysis:
Synchronous Satellite to Synchronous Satellite
(600 Mb/sec)

Parameter	Value (dB)
Transmitter Power	0
Transmitting Antenna Gain	97
Transmitting Losses	-2
Pointing and Conical Scan Losses	-1
Space Loss	-276
Receiving Antenna Gain	99
Receiver Losses	-3
N_o	-190
B	-88
CNR	16
Required CNR	13
Margin	3

STATE-OF-THE-ART

Introduction

In this last section of our paper we examine the characteristics of the existing hardware for spaceborne CO_2 laser systems. First, a brief tour of the major system blocks in a CO_2 laser transceiver is in order. Figure 7 shows a greatly simplified block diagram. Consider first the receive path. Energy from the opposite terminal strikes a gimballed flat mirror, called the coarse-pointing mirror in the subsequent discussion, and is directed through the telescope which serves as the receiving antenna. Two fields of view are important to our discussion: first, the field-of-view determined by the coarse pointing mirror and the usable image-plane dimensions of the telescope and, second, the instantaneous field-of-view of the telescope. The first controls the solid angle to be scanned in the acquisition process and the second controls the antenna gain pattern dimensions or the resolution of the telescope.

Behind the telescope in the receive path is the image motion compensator (IMC). This device is a piezoelectrically controlled beam steerer which controls where the instantaneous field-of-view is within the overall field-of-view of the telescope. Referring back to our previous discussion on acquisition, the instantaneous field-of-view was the 40 microradian number, while the overall field-of-view was the 0.2° number. The objective of the acquisition and tracking process is to superimpose the instantaneous field-of-view on the received signal's image. The IMC is used to scan the overall field-of-view during the initial search and to receive tracking corrections afterwards. When the IMC nears the end of its maximum range of deflection (typically 1° which, because of the magnification of the telescope translates into nominally 0.1° ahead of the telescope), a signal is supplied to move the coarse pointing mirror until the IMC is recentered in its range.

After the IMC the received energy passes the diplexer, which separates the transmitted and received energy, and reaches the nutator. The nutator is identical to the IMC, and indeed the functions can be combined in a single unit, and imposes a circular nutation on the received signal. This nutation is then used to generate a tracking error signal. Following the nutator, the local oscillator (LO) laser beam is inserted and both the received signal and LO beams impinge on the infrared mixer where a difference signal is generated. The intermediate frequency is the algebraic difference of the LO frequency and the Doppler frequency, which in the LAS-SRS link may vary ±700 MHz.

Because of restrictions in the tunability of currently available laser LO's which prohibit complete Doppler tracking with the laser LO, a double-conversion receiver is employed as shown in Figure 8. In this receiver the Doppler frequency

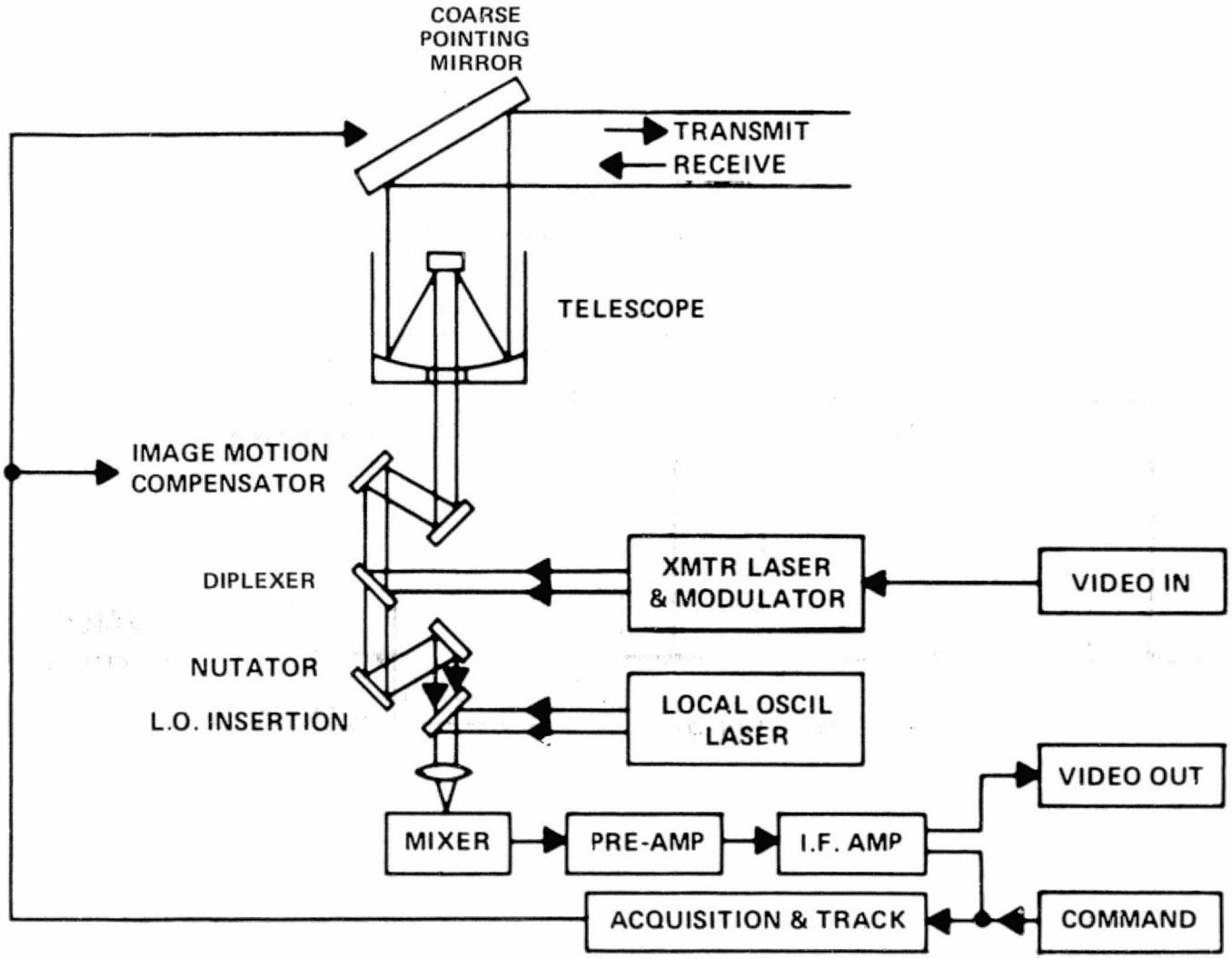

Figure 7. Simplified Block Diagram of Laser Heterodyne Transceiver

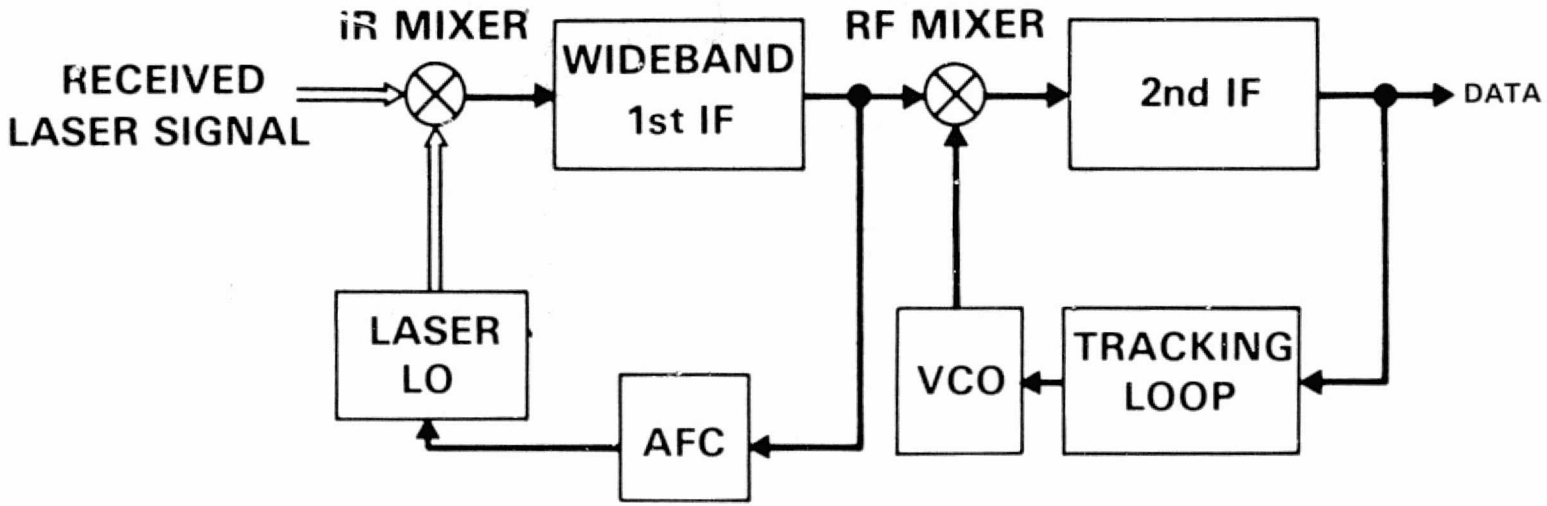

Figure 8. Double-Conversion Laser Heterodyne Receiver

is tracked in the second loop by an RF voltage-controlled oscillator (VCO). The operation can be visualized by means of the chart shown in Figure 9. In (a) the received signal is at the peak positive Doppler, +700 MHz, and the laser LO is set at +300 MHz, both with respect to the laser's center frequency. As the Doppler decreases, the automatic frequency control loop maintains the second IF at 400 MHz. When zero Doppler is approached, the laser LO is approaching -400 MHz and data foldover is imminent. At that point, the laser LO is switched to +400 MHz and AFC tracking continues as the Doppler frequency takes on negative values with respect to the center frequency.

Returning to the transmit path, modulated laser energy leaves the laser transmitter, is diplexed with the receive path, and passes through the IMC, telescope and coarse pointing mirror to leave the terminal. If the point-ahead angle is large in comparison to the transmitted beamwidth, a point-ahead compensator, identical to the IMC, is inserted in the transmit path between the laser transmitter and the diplexer.

Receiver Engineering Model

The receiver was regarded as having the greatest potential for difficulty and was, consequently, addressed first. The objective was to develop a complete engineering model that would accurately reflect all functions of a flight model and, in critical areas, reflect the actual flight equipment configuration. The critical areas were identified to be the optical-mechanical assembly, the coarse pointing and fine tracking assemblies, the radiative cooler needed to cool the infrared mixer to its operating temperature below 120°K, the infrared mixer itself, and the laser LO. The electronics subsystems were not regarded to be as critical and, therefore, rack-mounted electronics having the appropriate functional characteristics were developed.

The optical-mechanical assembly is shown in Figure 10(a) with the front cover in place and in 10(b) with it open to reveal the primary mirror (on the left) and the coarse pointing mirror (on the right). In this optical configuration, the secondary mirror is behind the coarse pointing mirror. The received energy is first directed to the left by the coarse pointing mirror and then focused by the primary mirror through a hole in the coarse pointing mirror to reach the remainder of the optical system. Figure 11 shows an artist's cut-away view of the optical system.

The optical system is an all-reflective folded Gregorian configuration with an 18.5 cm (7.3 in.) diameter primary mirror which gives a 93 dB antenna gain at ten micrometers. This configuration was chosen because it has zero spherical aberration on-axis and neglibible coma and astigmatism off-axis. The specification for the antenna gain was met over a 0.26° field-of-view so that off-axis

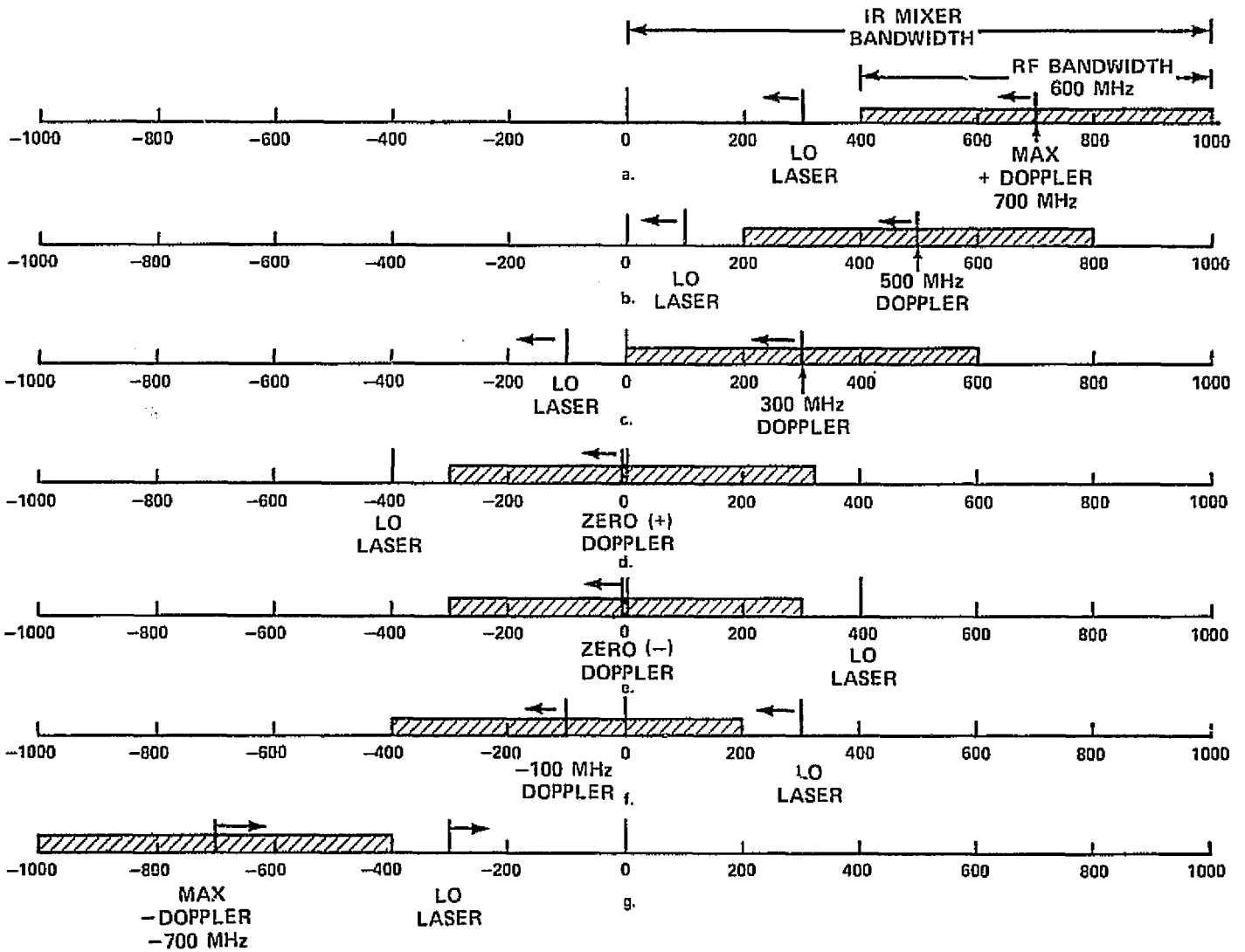

Figure 9. Doppler Tracking Sequence

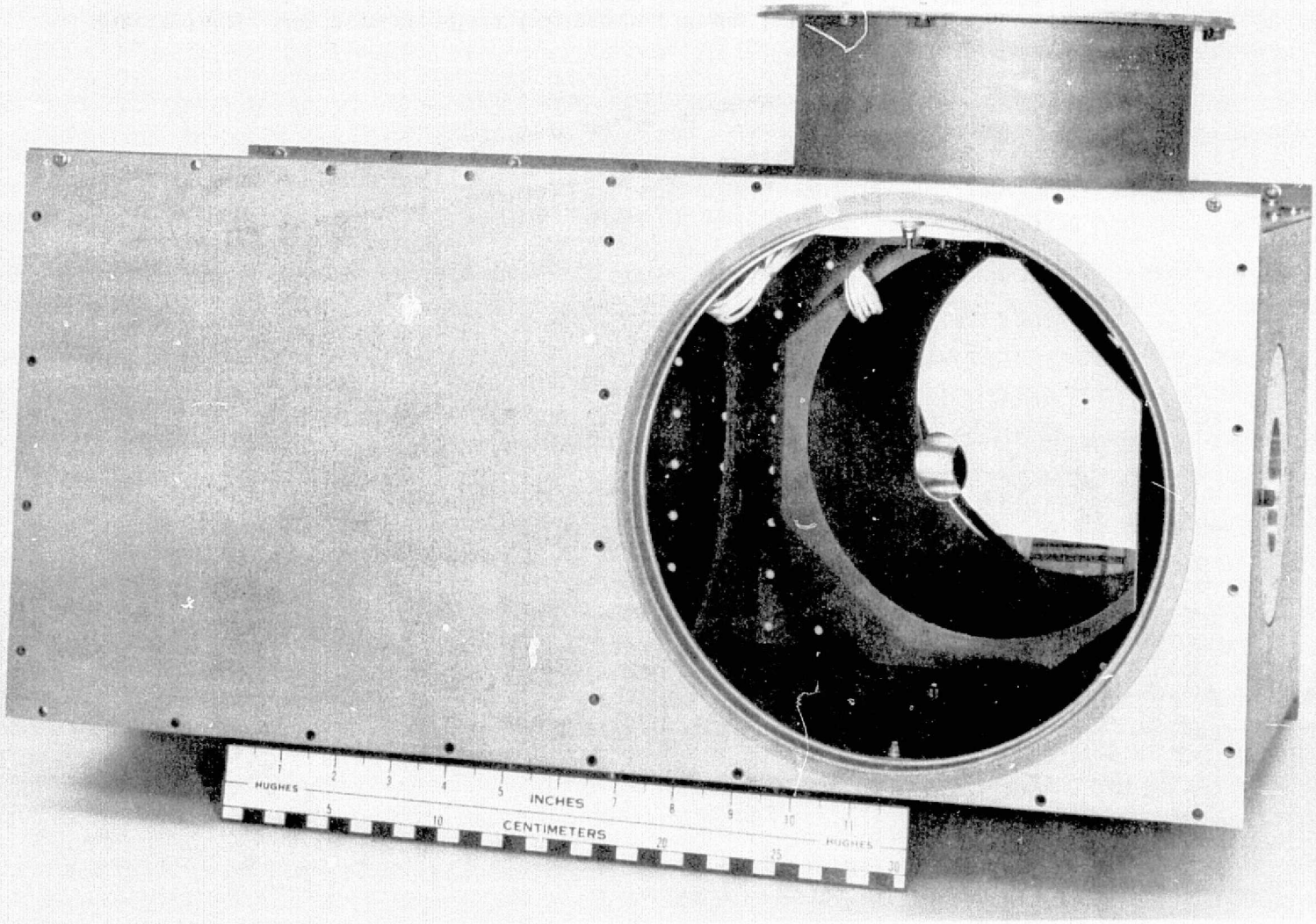

Figure 10(a). 300 Mbps Receiver Engineering Model Front View

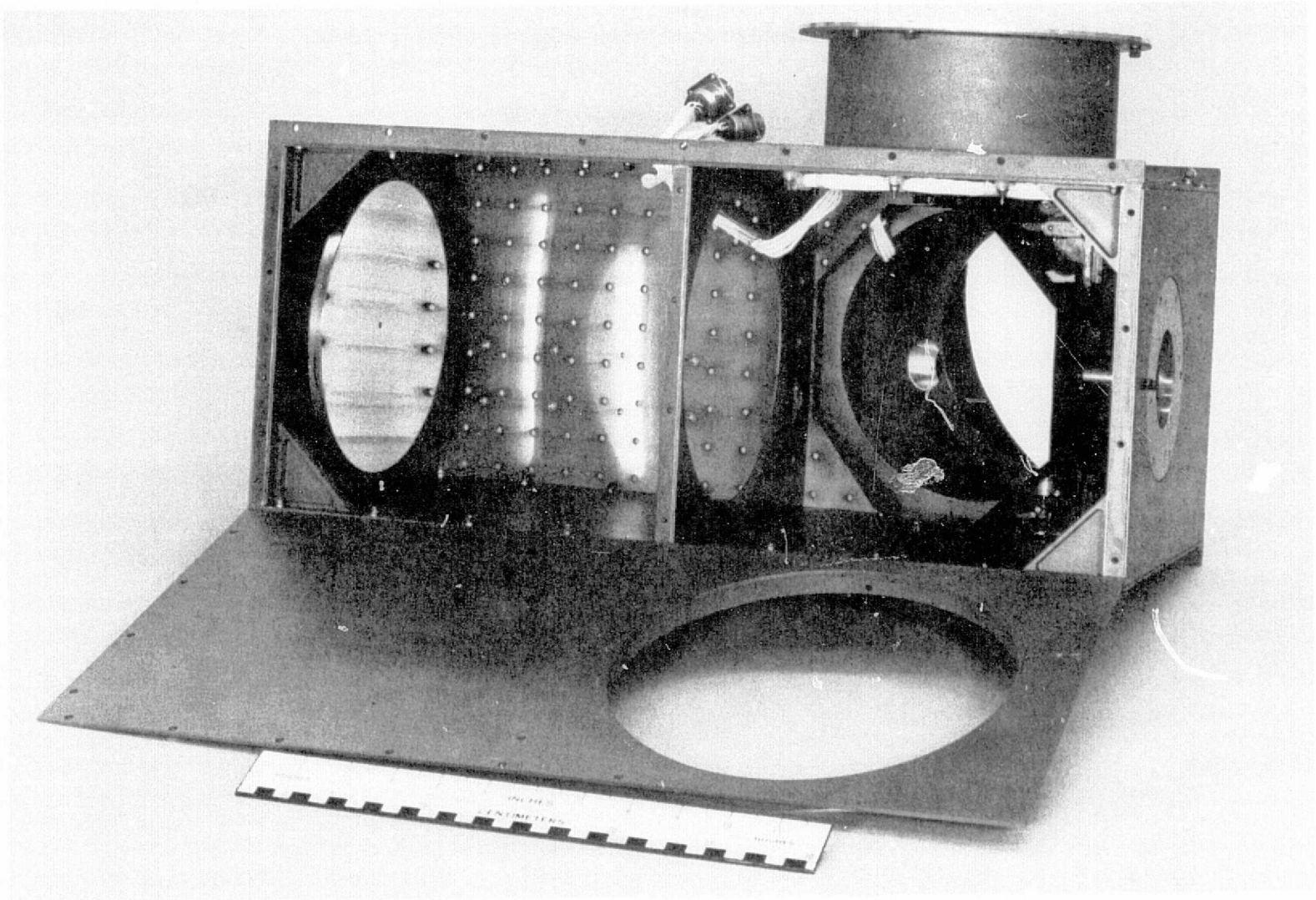

Figure 10(b). 300 Mbps Receiver Engineering Model Front View with Cover Removed

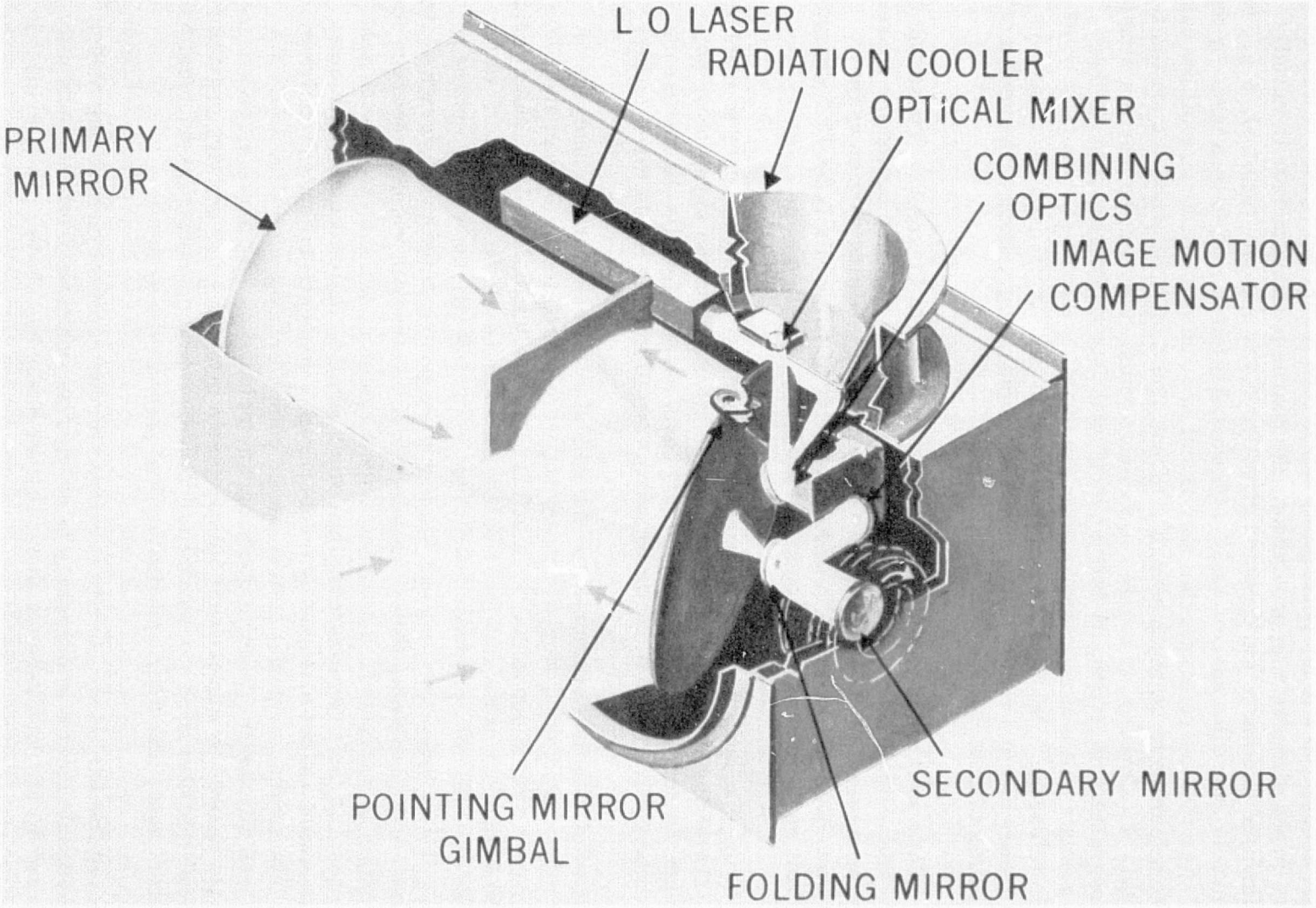

Figure 11. 10.6-Micrometer Laser Heterodyne Receiver Optical Layout

signal acquisition was not perceptibly worse than the on-axis case. As noted above in the discussion on acquisition, the coarse pointing mirror is initially commanded to point in the expected direction of the opposite terminal, e.g., to an initial error allowance of ±0.1°. The acquisition search is then made by the IMC over that entire range; this may result in acquisition occurring off the axis of the telescope by as much as 0.1°. Hence, good off-axis performance is essential. Incidentally, it is this requirement which rules out the use of a simple Cassegrainian telescope. A further incidental, but important, point is that there exists only one optimum location for the IMC; that point is the exit pupil of the telescope. Deviations from that location rapidly produce increased system losses due to a tilting of the signal beam (see, e.g., Ross's discussion of the tilting effects[19]).

The IMC's used in the engineering model are shown in Figure 12. These units were space-qualified on a previous program and are mounted behind the coarse pointing mirror.[20] The particular IMC's used, a modified version of the Sylvania PBM-8G, have a deflection parameter of nominally 7.8×10^{-4} degrees per Volt and a resonant frequency of 1200 Hz.

Following the IMC's is a flat mirror with a small hole which is used to combine the LO and signal beams. The LO laser is injected into the signal beam path through the small hole, while the signal beam essentially fills the mirror and is reflected by it. The two collinear beams then illuminate the infrared mixer.

In parallel with the development of the optical system, extensive analyses of heterodyne receiver optical requirements were completed by Degnan and Klein[5] and Brewer and Nussmeier.[21] In brief, those analyses showed that the mismatch of the f-numbers of the two laser beams, f/8 for the signal beam and f/40 for the local oscillator, produces a 3 dB loss in mixing efficiency due to phase effects. While these results came too late to be incorporated in the design of the present optical system, they illustrate one of the areas in which a generous dose of caution is warranted. Laser heterodyne systems, while no more stringent in general in their requirements than other laser optical systems, have other needs which are not necessarily evident from a conventional optical analysis. For this reason, a special optical design computer program called LACOMA has been developed. This unique program includes phase effects which are frequently ignored in conventional optical design programs and includes provision for multiple apertures (to account for the separate transmitter laser, local oscillator laser, and other principal optical paths in the system).

A waveguide CO_2 laser LO was developed for the receiver engineering model.[22] A waveguide laser was necessary to provide the enhanced frequency tunability required by the double-conversion receiver described above. As is evident in

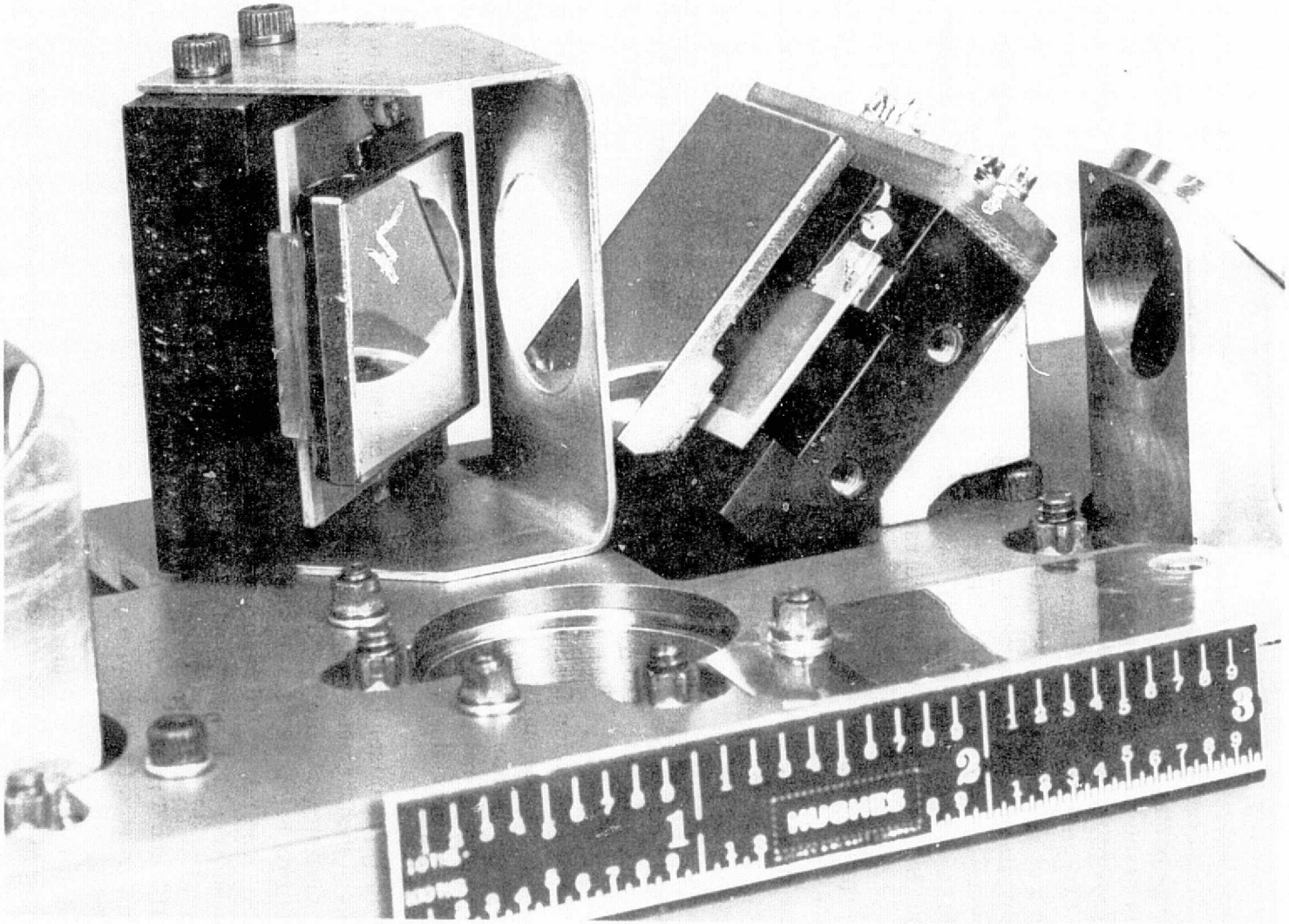

Figure 12. Fine Beam Pointing Mirrors and Piezoelectric Drive (IMC)

Figure 9, the minimum required tunability is equal to the IF bandwidth, i.e., twice the highest baseband frequency. The laser presently being used in the receiver has a beryllium oxide circular bore which is 1.5 mm in diameter. Four discharge sections are used (as shown in Figure 13(a)) in order to reduce the discharge voltage to approximately 2.4 kV. Figure 13(b) shows the discharge paths; the advantage of this arrangement is that the electrodes at the ends of the tube are at ground potential. A diffraction grating serves as one mirror of the laser and restricts operation to only the desired spectral line of the CO_2 molecule. The desired IF is obtained by use of a Stark cell stabilization technique described by Nussmeier and Abrams.[23] Voltage tunable resonant absorption of CO_2 laser radiation in deuterated ammonia (NH_2D) is exploited to produce a tunable frequency discriminant. The absorption dip is nominally 80 MHz wide and can be used to stabilize the LO laser (long-term) to better than ±100 kHz over the entire tunable range of the LO.

The waveguide laser LO and its Stark cell are shown installed on the back plate of the receiver engineering model as shown in Figure 14. These components were absent from the preceding photographs of the engineering model. This laser has demonstrated a line center power output of 540 mW, a 1 dB tuning range of ±200 MHz, a 3 dB tuning range of ±300 MHz, and requires an input power of less than 20 W. Tuning of the laser is obtained using a circular piezoelectric bender bimorph.[24] Extensive analyses of waveguide laser performance have been prepared by Degnan.[25,26,27]

A second generation LO laser is presently being developed and is specially designed for space qualification and life testing. A photograph of the first of the second generation LO's is shown in Figure 15. This design is more compact, more rugged, and requires half the input power that the earlier tube required,[15] while still providing adequate power output.

The infrared mixer used in the receiver engineering model was supplied to AIL under a subcontract by the French firm S.A.T. The mixer shown in Figure 16 is a mercury-cadmium-telluride (HgCdTe) photodiode and operates best at temperatures below 120°K. It was space-qualified by S.A.T. on a separate program. The mixer and its preamplifier have a frequency response from 5 to 1500 MHz, a 77°K noise equivalent power or NEP (P_N/B in the earlier discussion) of 10^{-19} W/Hz at 1500 MHz, and a 130°K NEP of 1.75×10^{-19} W/Hz at 20 MHz and 3×10^{-19} W/Hz at 1500 MHz. The measured NEP of the receiver front-end as a function of temperature and bias voltage is shown in Figure 17, while Figure 18 shows it as a function of temperature and frequency.[28] Cohen has developed a useful model of photodiode performance for systems analysis; it was produced in support of the receiver development program shown in Figure 1 and accurately predicts all significant functional dependencies.[29]

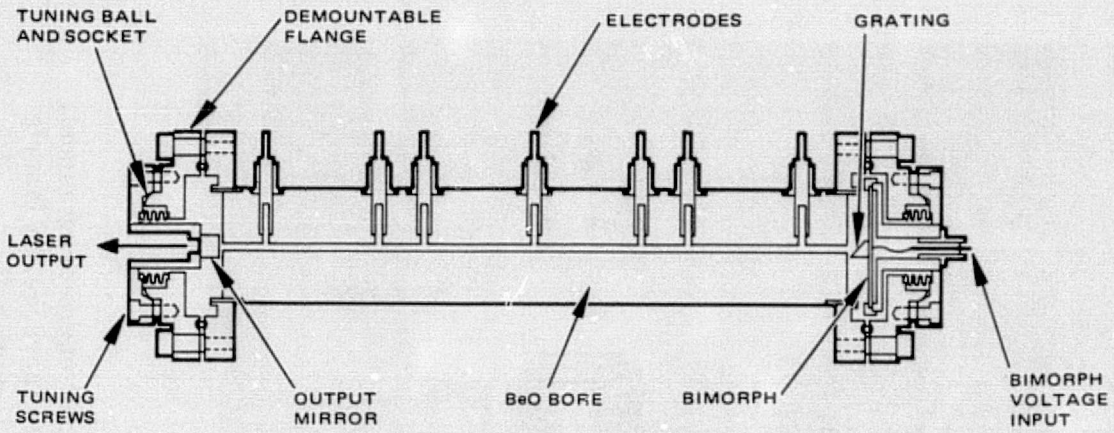

Figure 13(a). Waveguide Laser Detail

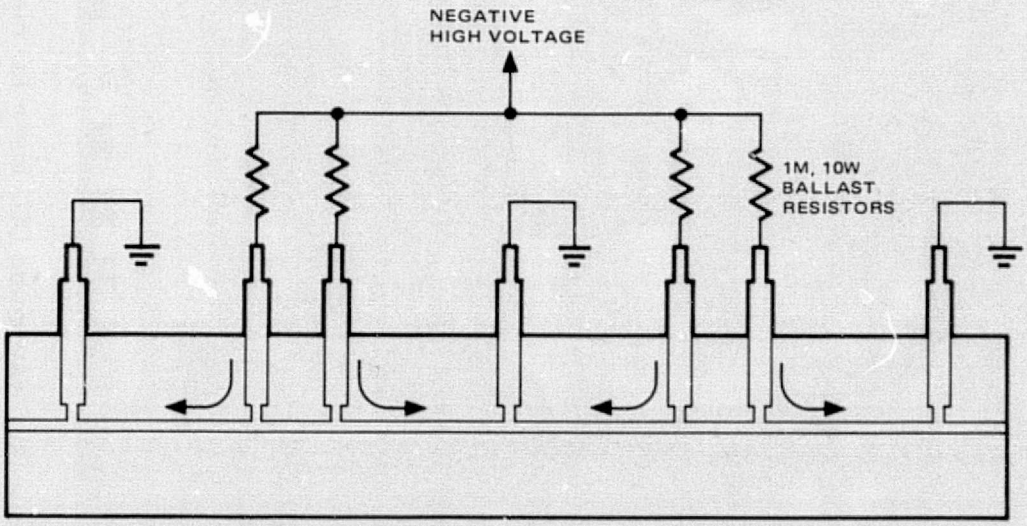

Figure 13(b). Electrode Arrangement for Exciting Four Separate Discharge Paths

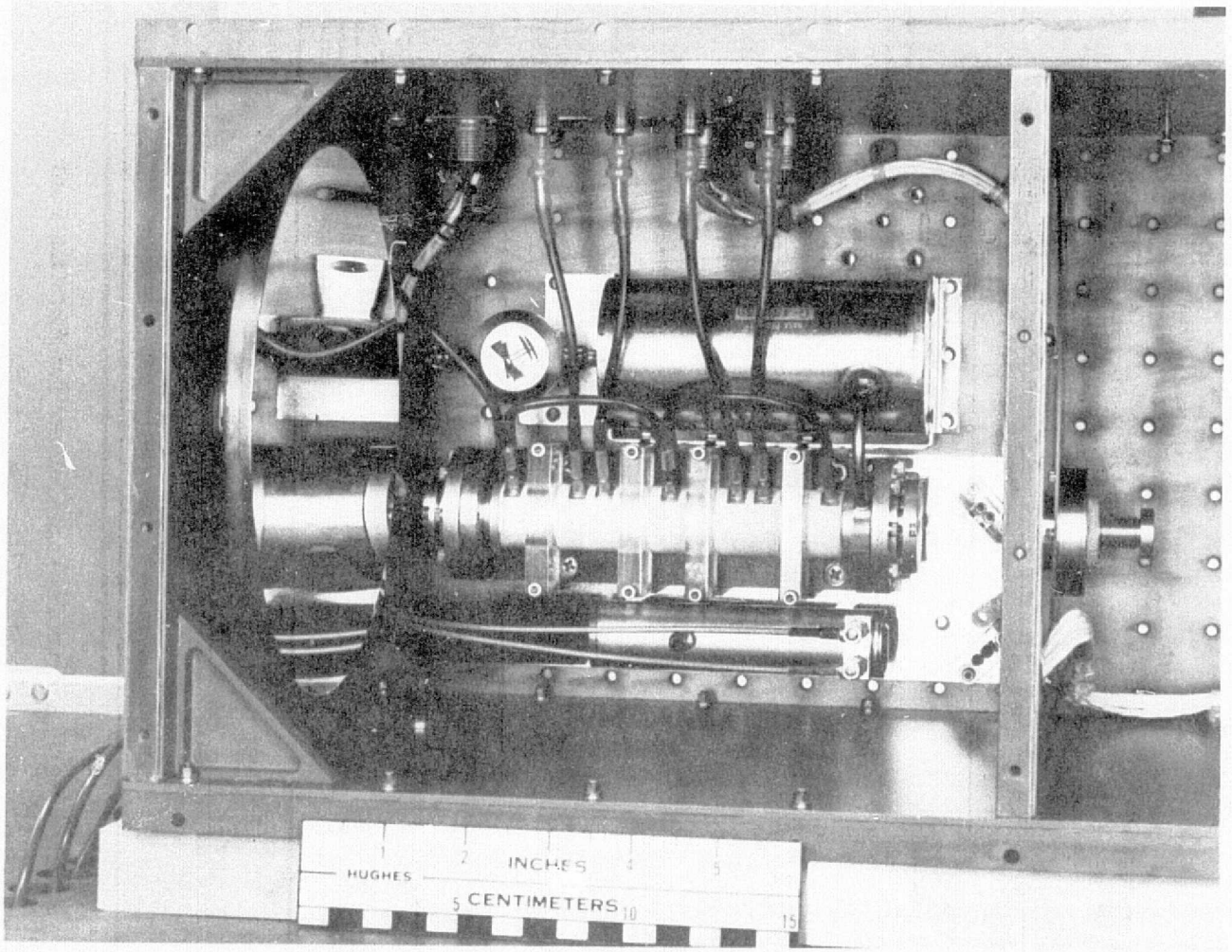

Figure 14. Waveguide CO_2 laser LO installed in the receiver engineering model. The cylinder above the laser is a ballast tank to increase the laser's gas volume. The smaller cylinder below is the stark cell.

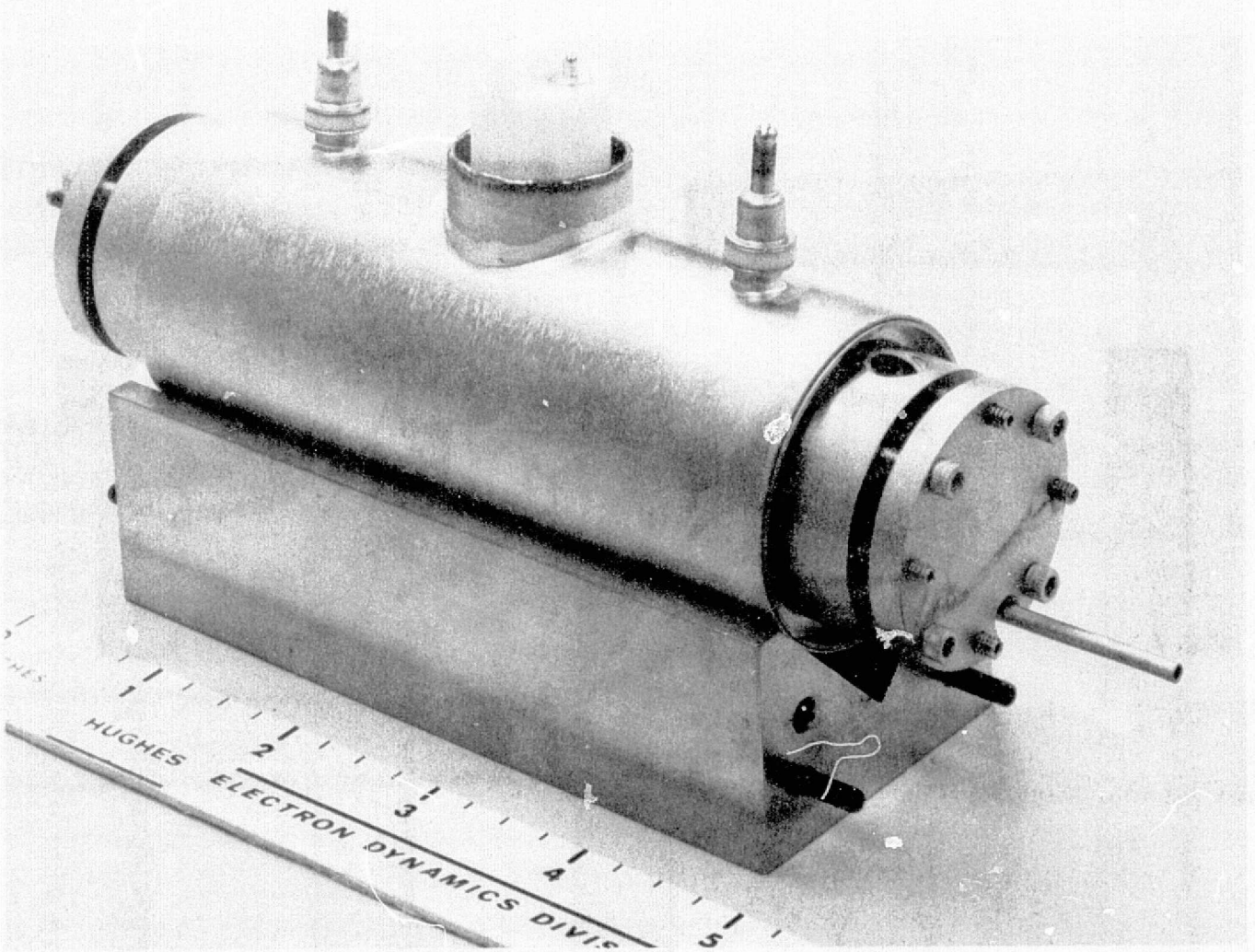

Figure 15. Second-Generation Waveguide CO_2 Laser Local Oscillator Designed for Space Qualification

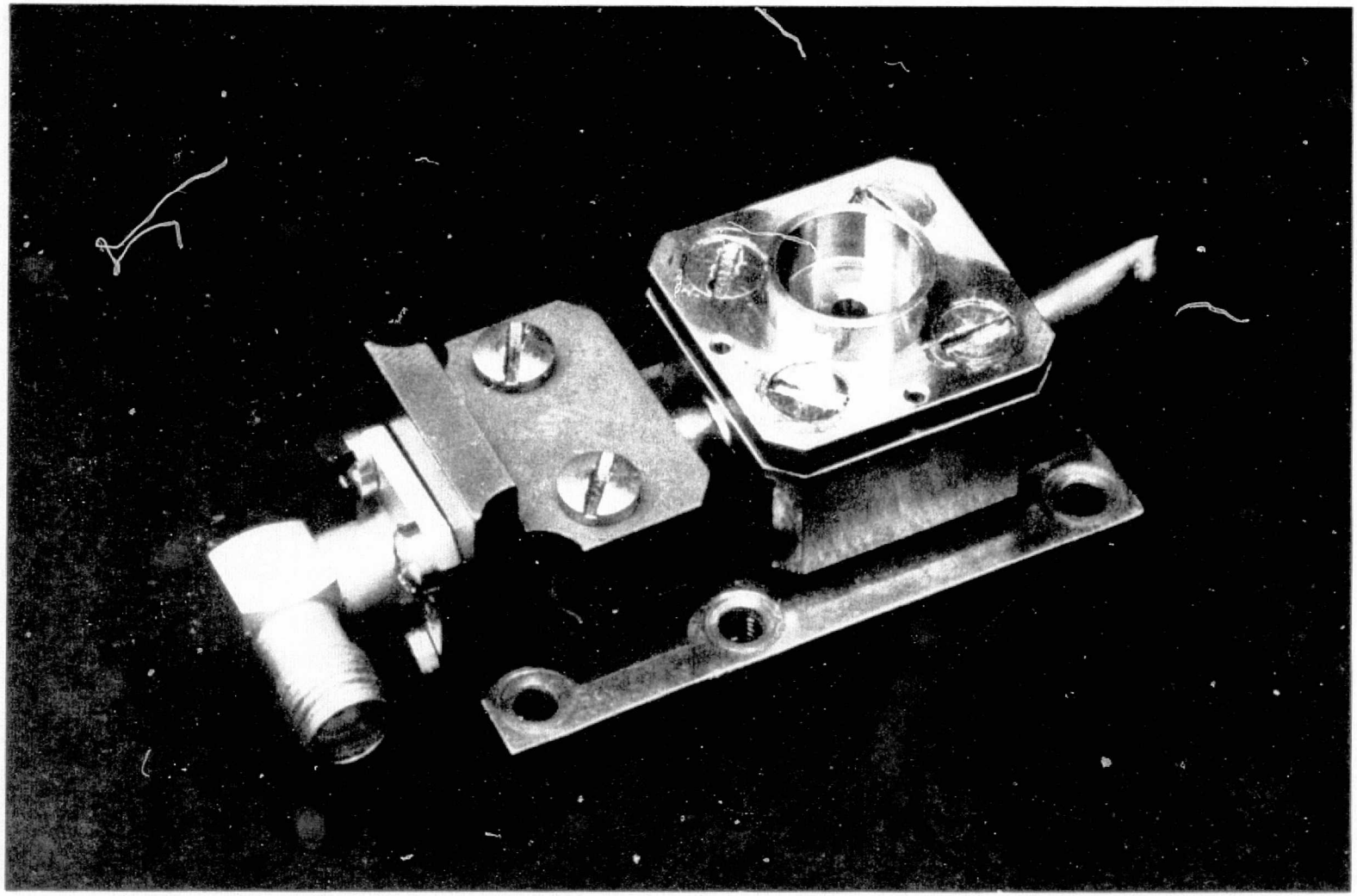

Figure 16. Space-qualified HgCdTe infrared mixer developed for NASA by S. A. T. The long dimension is approximately 4 cm.

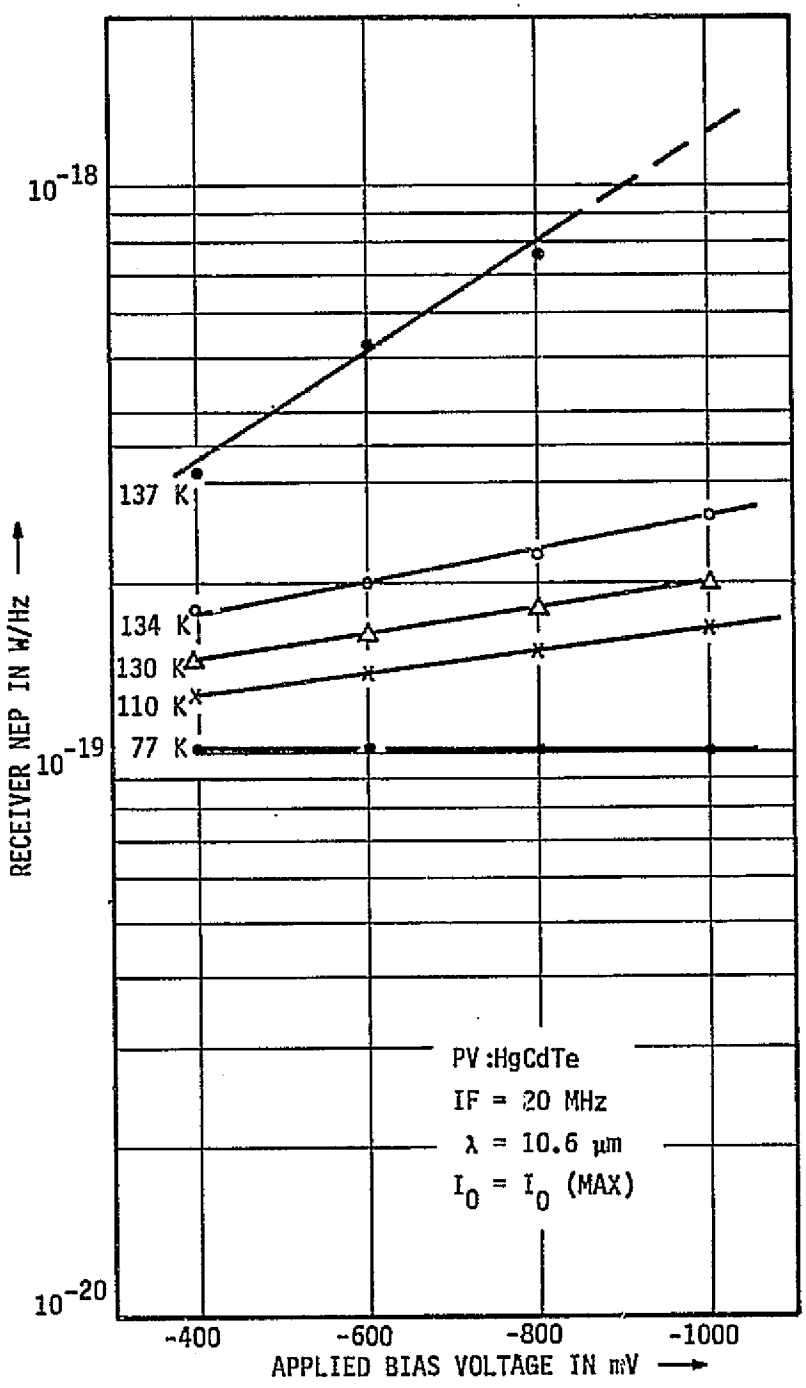

Figure 17. Measured Heterodyne Receiver Sensitivity as a Function of Applied Photomixer Bias Voltage with Photomixer Temperature as a Parameter

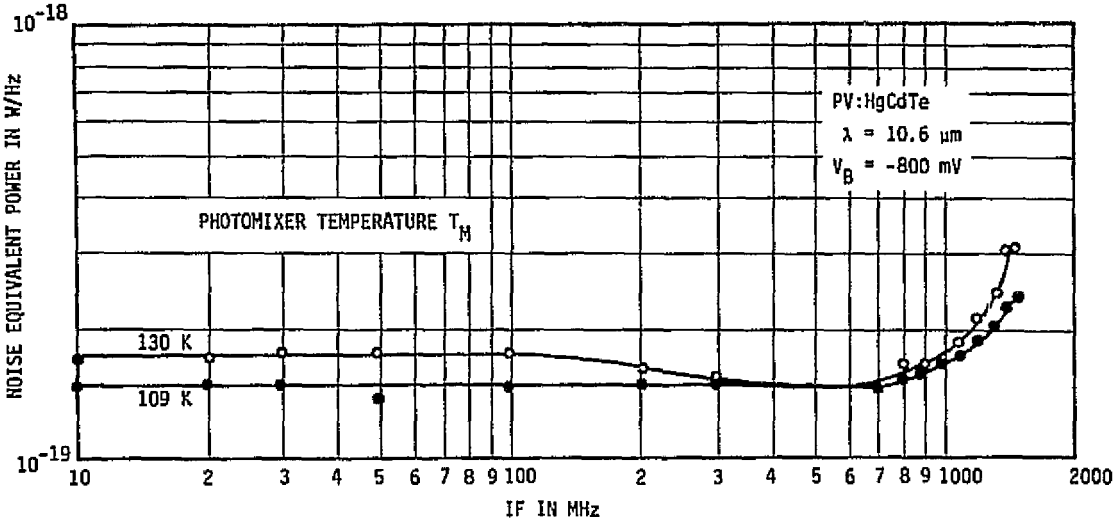

Figure 18. Heterodyne Receiver NEP Versus IF with Photomixer Temperature as a Parameter

The infrared mixer is cooled to its operating temperature by a radiative cooler developed by Arthur D. Little, Inc.[30] The cooler, shown in Figure 19, is a modification of a space-tested cooler and has been successfully subjected to a sequence of thermal-vacuum and vibration tests at flight acceptance levels. The cooler's support ring, mounted approximately midway down the sunshade, bolts to the cylinder on the top of the engineering model in Figure 10. The radiative cooler weighs 1.6 kg (3.5 lbs) and maintains the inner stage below 112°K in spite of an active thermal load (mixer bias power plus laser local oscillator power) of 40 mW. A total load of 20 mW results in an inner stage temperature of less than 107°K. The cooler requires a clear field-of-view to dark space of nominally 120°.

Having examined the mixer and its cooler, we will now review the circuits following the mixer. A number of tracking loop configurations were examined for use in the second loop of the double-conversion receiver; they included conventional phase lock loops which use the residual carrier in the demodulation process and other loops which use the modulation energy to either extract a carrier replica or enhance the signal-to-noise ratio in a standard loop. Of these alternatives, the "squaring loop" was chosen on the basis of efficiency and ease of development.[32] Figure 20 shows a simplified block diagram of the squaring loop.

The signal from the preamplifier is passed through a linear phase bandpass filter with a 400 MHz 3-dB bandwidth. It is then split into two paths, one path goes to the data demodulator and the other serves to provide the tracking loop

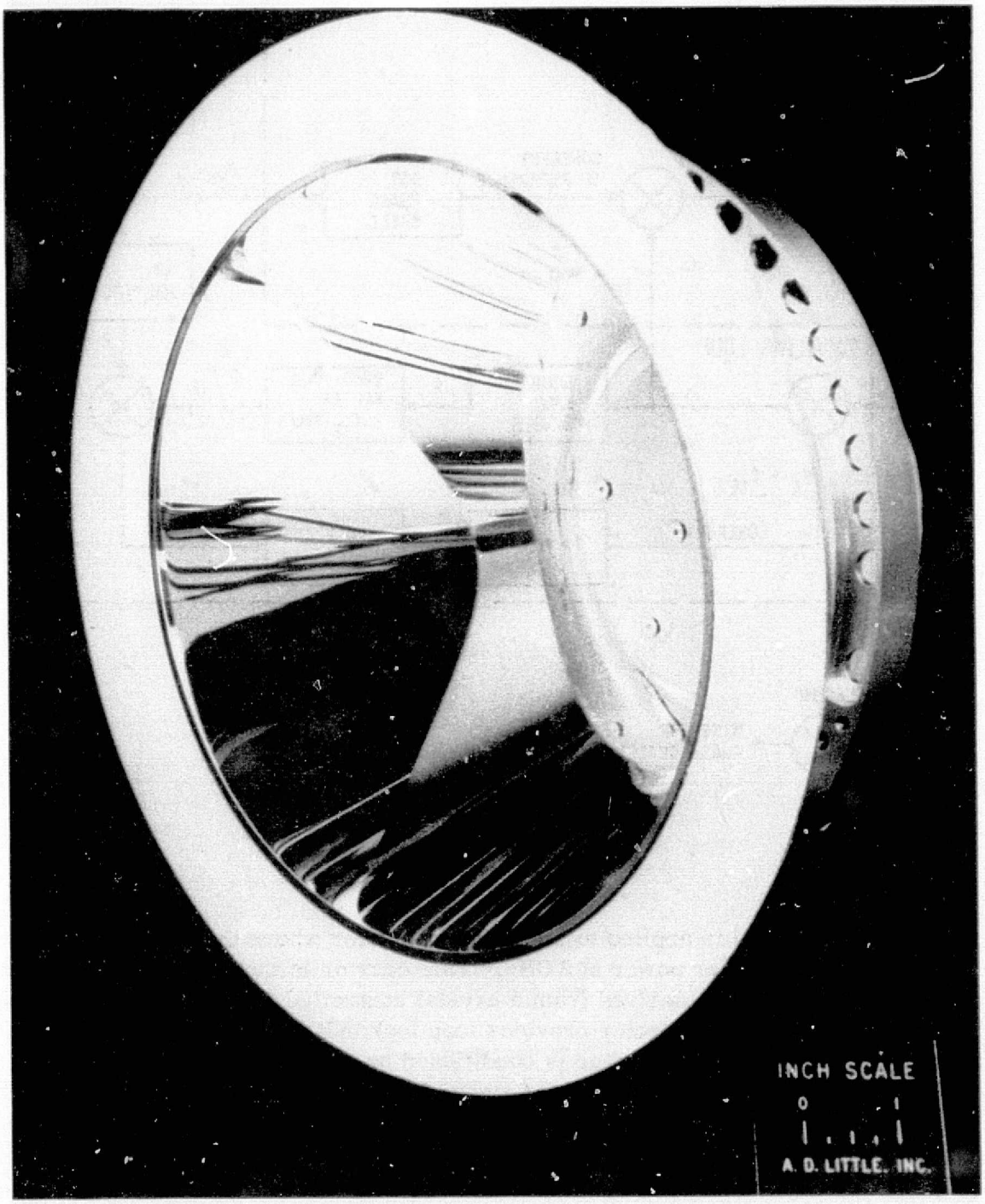

Figure 19. ADL Radiative Cooler

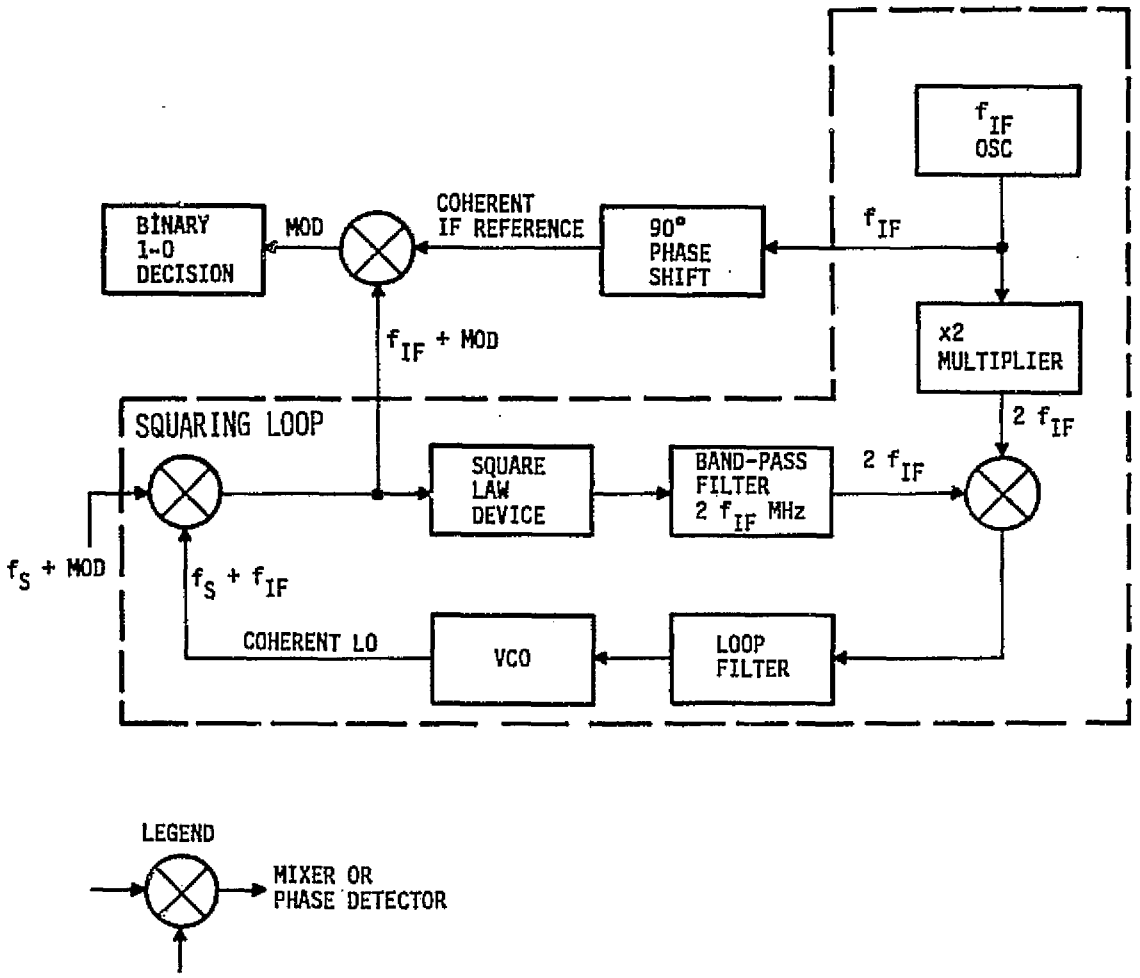

Figure 20. Squaring Loop

signal. The second is applied to a frequency doubler where the sideband energy is converted to carrier power at 3 GHz. This carrier is then compared in phase with a 3 GHz reference derived from a crystal controlled reference source. The quadrature loop phase detector provides loop lock indication. The error voltage from the loop phase detector is conditioned by the loop filter and amplifier so that the VCO tracks the modulated signal frequency. The 1500 MHz reference is also applied to the data demodulator so that, when the loop is locked, the two inputs to the data demodulator have the proper phase to demodulate the signal. Figure 21 shows the measured performance of the Doppler tracking receiver back-end. The increasing error rate at lower IF's (designated f_s in the figure) are the result of a signal image frequency and VCO leakage power. It can be seen that, at the design IF of 400 MHz, the receiver is operating within 3 dB of theoretical. These measurements were made with a Tau-Tron Inc. S-1000-A bit error rate test set.

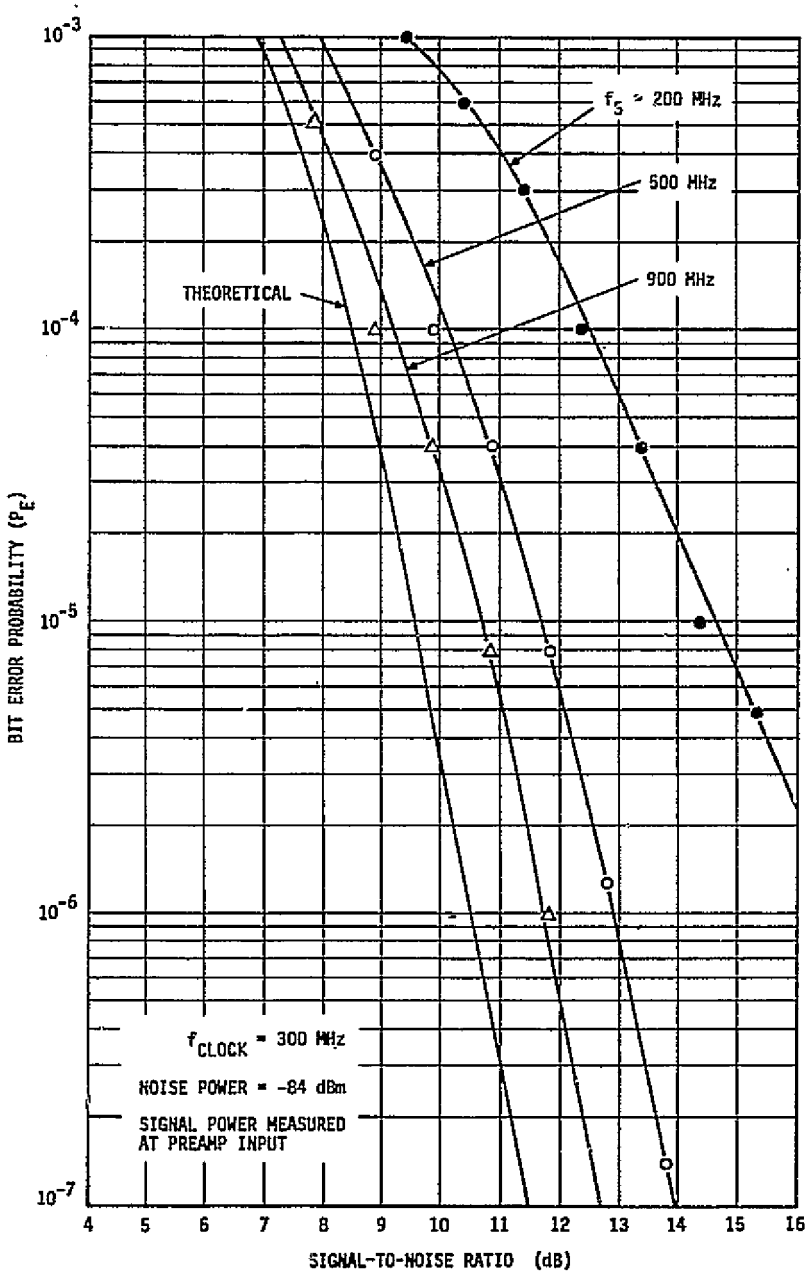

Figure 21. Measured Bit Error Probabilities

We continue our discussion of the receiver engineering model by examining the optical-mechanical subsystem characteristics and some of the supporting analyses which give confidence that a flight-worthy unit could now be developed. An extensive thermal analysis was conducted on the beryllium structure. The analysis shows that the optical-mechanical subsystem operates with negligible distortion even when exposed directly to sunlight or when the sun is imaged on the coarse pointing mirror by the primary mirror. The worst-case thermal distortion is only 1.5%. This result, plus the insensitivity of the ten micrometer receiver to the solar radiation—because of its comparatively low power spectral density at ten micrometers[31]—permits the receiver to operate while tracking the signal across a solar background.

A structural analysis, arranged to closely match the thermal model, was also performed. Analytical results were obtained for static 1 g loading and dynamic sinusoidal sweep loading of the structure. The former case showed no signal loss. In the latter case, the lowest mechanical resonance is on the order of 617 Hz, which is well above that considered structurally dangerous. Also, the worst-case loads produced maximum stresses only one-tenth of the material stress limit. The vibration profile assumed in the analysis was that required for the ATS-6 satellite, which is representative of any modern geosynchronous communication satellite.

The optical-mechanical subsystem has rectangular dimensions of nominally 25.4 x 25.4 x 54.6 cm (10 x 10 x 21.5 in.), not including the support cylinder for the radiative cooler or the cooler itself, and the subsystem weighs 11.3 kg (24.8 lbs).

Lubrication in space is always of concern and special concern has been taken in the development of the coarse pointing mirror assembly. The overall characteristics of the assembly are given in Table 4 and a photograph with the assembly removed from the structure is given in Figure 22. Coarse pointing of the flat pointing mirror is obtained by a two-gimbal assembly. The flat mirror is mounted in a yoke on a rotatable pedestal. Rotation of the pedestal provides azimuth (or roll) sweep, while elevation sweep results from declination or tilt about the mirror's pivot axis in the yoke. Positioning is independent in each axis and performed by a space-qualified stepper motor drive. The positioning drive for each axis consists of a spur gear reduction from the motor shaft to a final single thread worm gear engaged in a matching worm wheel. These gears are lubricated with a dry film suitable for space use which will not migrate to optical surfaces or boil off in vacuum.

One of the parameters strongly influencing the design of both the acquisition and tracking subsystems is the maximum target angular rate. This rate is the sum

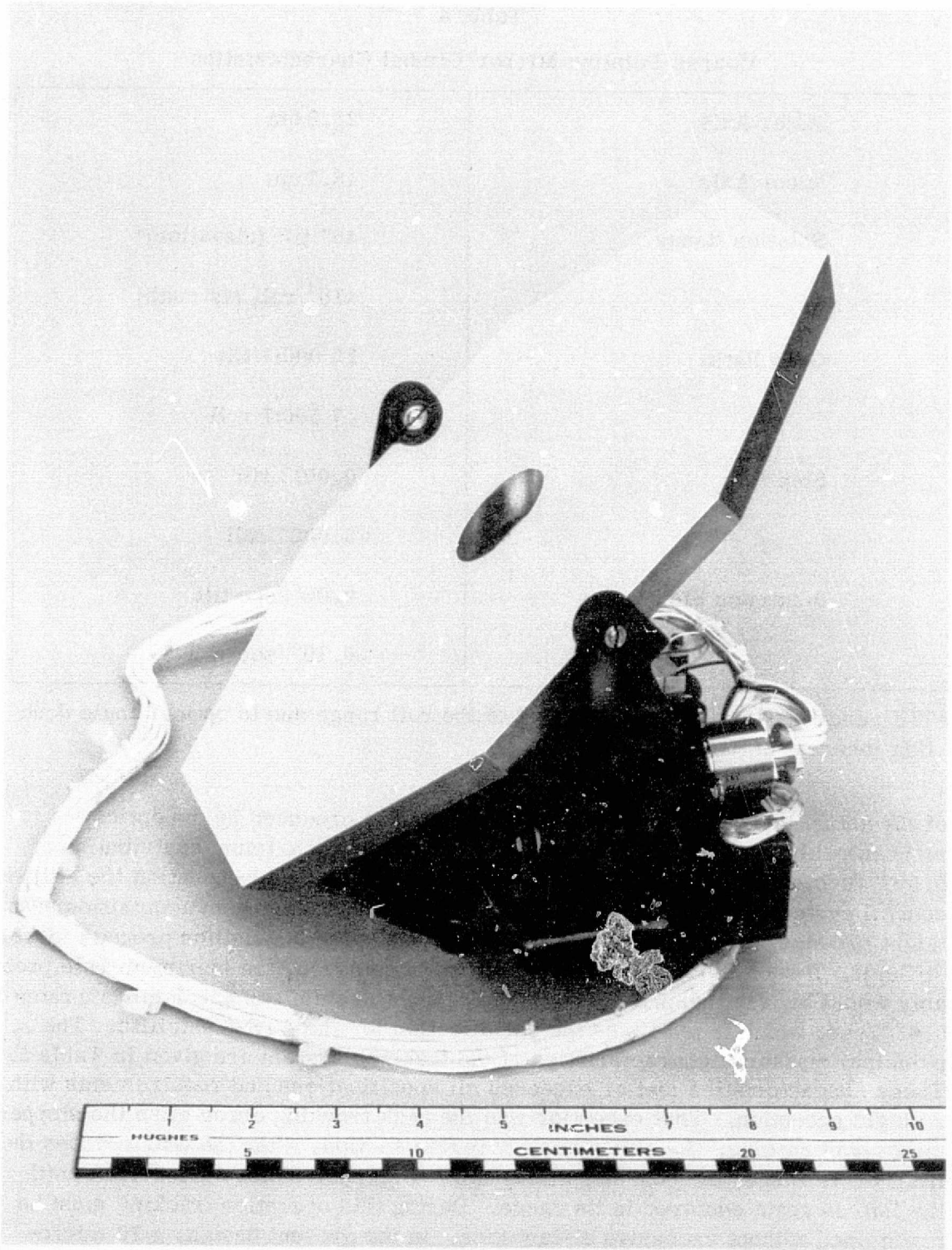

Figure 22. Coarse Pointing Mirror Gimbal Assembly

Table 4

Coarse Pointing Mirror/Gimbal Characteristics

Major Axis	28.3 cm
Minor Axis	18.1 cm
Rotation Range	±5° tilt (elevation)*
	±10° roll (azimuth)
Gear Ratio	15 000:1 tilt
	7 500:1 roll
Step Size	0.001° tilt
	0.002° roll
Maximum Slew Rate	0.05°/sec tilt
	0.10°/sec roll

*Tilt range needs to be only half that of the roll range due to optical angle doubling inherent in the tilt axis.

of the actual target motion and the angular motion produced by the optical-mechanical base. The LAS-SRS mission produces a maximum contribution of 0.007°/sec. The angular motion of the base is strongly dependent on the attitude control system of the SRS, e.g., firing a reaction jet during an acquisition scan might produce a 0.1°/sec rate, which would make the acquisition process more difficult. If such firing is prohibited during acquisition, the maximum rate probably would be less than 0.01°/sec. The present system can accommodate rates of 0.03°/sec, which is ten times the specification for the ATS-6 satellite. The principal measured characteristics of the tracking system are given in Table 5. These characteristics met or exceeded all specifications and requirements with a single exception. That exception was the peak tracking error when the stepper motor was running. As stated earlier in this section, when the IMC reaches the limit of its range, the coarse pointing mirror stepper motors are driven until the IMC is again centered in its range. During this operation tracking must be maintained without excessive disturbance. In the present design, a 70 microradian error occurs during stepper motor operation and produces an unacceptable signal loss during communication. A necessary modification, therefore, in

Table 5

Measured Tracking System Performance Data

TRACKING LOOP	
Static Tracking Error	7 microradians
Tracking Error Due to 0.03°/sec Target Motion	3.5 microradians
Peak Tracking Error with Stepper Disturbance	70 microradians
Tracking Loop Bandwidth	50 Hz
Acquisition Field-of-View	0.2° x 0.2°
Acquisition Time	Less than 1 minute
Maximum Target Velocity for Acquisition	0.3°/sec
IMC LOOP	
IMC Noise Level	7 microradians
Pointing Accuracy	7 microradians
IMC Bandwidth	405 Hz

the production of a flight model based on this design would be to reduce the step size applied to the mirror and to increase the step rate to compensate for the smaller step. Since the stepper motors are operating well below their maximum ratings, the modification would be straightforward.

To conclude our discussion of the receiver engineering model, we provide the brief summary of its principal characteristics given in Table 6.

Transceiver Engineering Model

The transceiver is a modification of the receiver engineering model by the addition of a 300 Mbps transmitter channel. Although a beacon laser is an essential element in an operational receiver, it was omitted from the receiver engineering model in anticipation of the later conversion. In the transceiver, the transmitter serves a dual function and acts as the beacon as well as its normal function.

Table 6

Receiver Engineering Model Characteristics

Intended Mission	Synchronous Satellite Data Receiver
Data Rate	300 Mbps
Doppler Tracking Capability	±700 MHz
Weight (not including electronics or beacon laser)	12.7 kg (28 lbs)
Power Requirement (not including beacon laser)	50 W
Tracking Field	20° x 20°
Initial Pointing Requirement	±0.1°
Acquisition Time	Less than 1 minute

There are three principal areas involved in the addition of the transmit function to the receiver: (1) the transmitter laser and its intra-cavity electro-optic modulator, (2) the modulator driver and coding format, and (3) the technique for transmit-receive diplexing. We will now examine each in that order.

The transmitter laser is similar in design to the LO laser in that it is a waveguide laser which uses metal-ceramic construction. The bore material is beryllium oxide for the same reasons as in the LO, namely its high thermal conductivity which permits efficient conductive cooling of the laser and its low waveguide loss at ten micrometers. It may have been noted in Figure 10(b) that the rear wall of the receiver engineering model has a grid of tapped holes. This is the surface to which all of the high power dissipators are mounted and the surface which connects the terminal to the spacecraft's heat sink. In the design of the terminal it has been assumed that the spacecraft maintains this surface at 20 ±15° C in spite of the thermal loads attached to it. The high dissipation loads are principally the lasers, high voltage power supplies, and the modulator driver. Figure 23 shows an artist's conception of the transceiver with the transmitter and LO lasers mounted on the rear wall.

Figure 24 shows a simplified drawing of the laser transmitter and its modulator crystal. As in the laser LO, the discharge region is divided into sections to

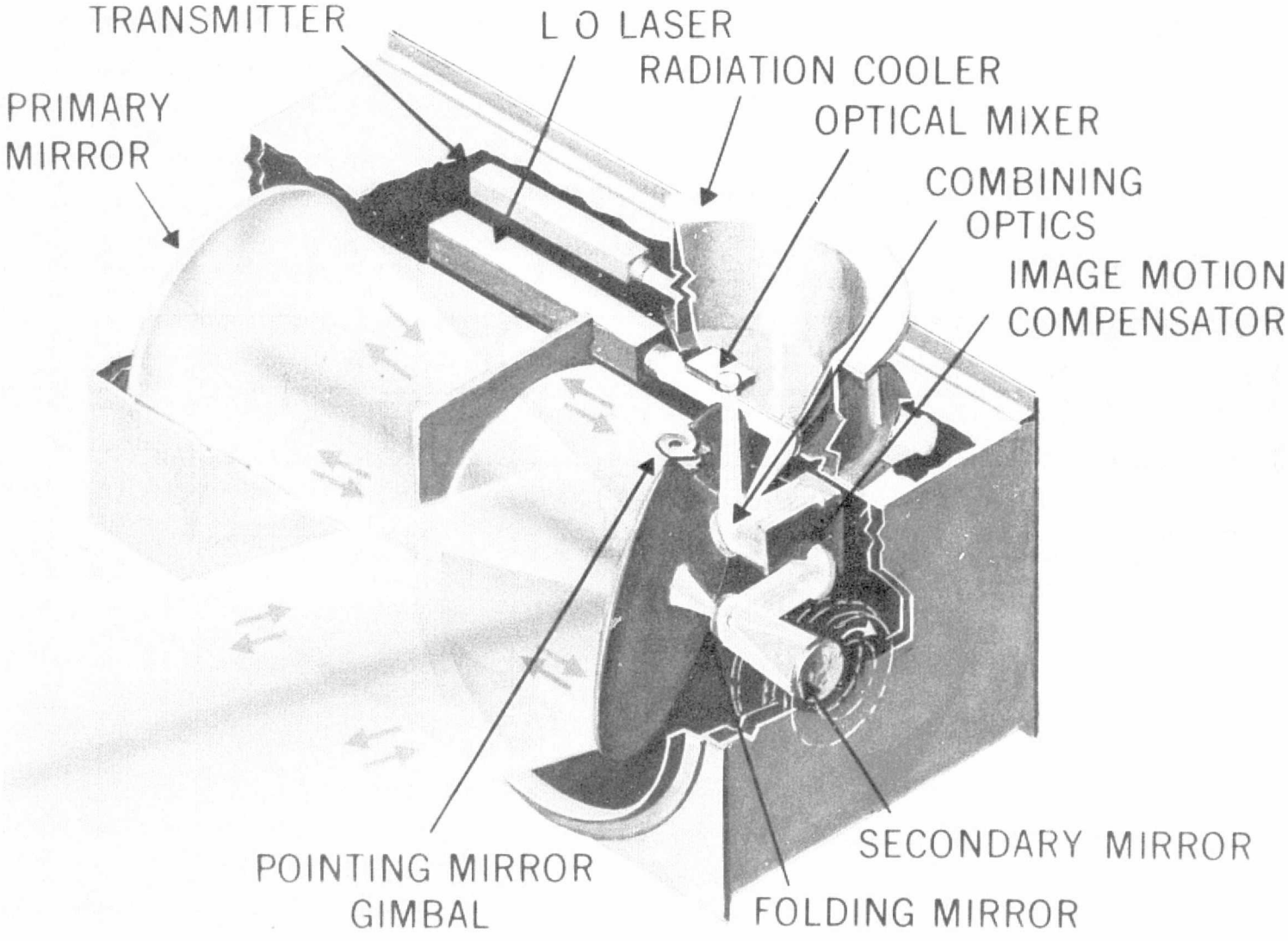

Figure 23. Artist's Conception of the Transceiver

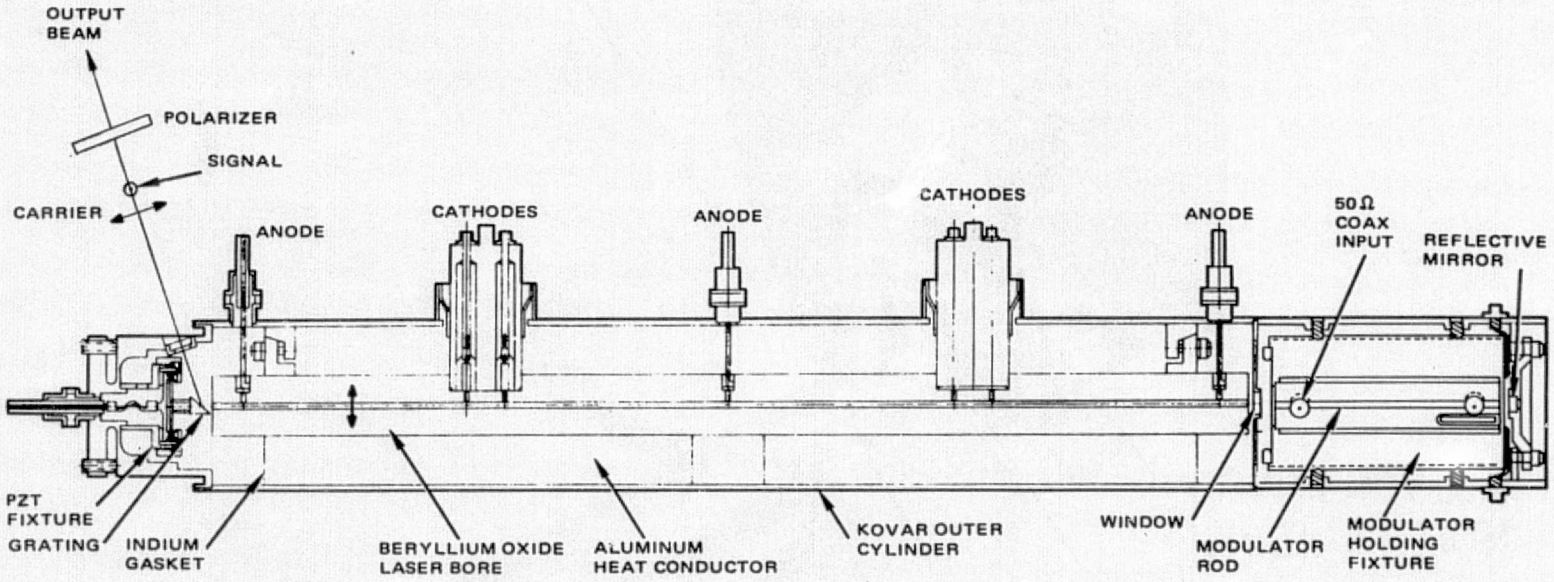

Figure 24. Section Drawing of Laser Transmitter

reduce the high voltage requirements. The laser bore is 26 cm long (of which 24 cm is useful discharge length) and is square in cross-section with 1.5 mm sides. The modulator is a cadmium telluride crystal 60 mm long, also with a 1.5 mm square cross-section. The laser discharge requires 55 W and, with 90 W supplied to the modulator crystal, a modulated power output of 0.7 W (of sideband power) is obtained. A residual, orthogonally polarized, carrier power of 0.25 W is also present in the output.

The modulator driver remains one of the more difficult areas of the system. The present approach to developing the required 120 V peak-to-peak modulator drive voltage is shown in Figure 25. The outputs from current mode logic driver modules using selected MSC 80041 transistors are combined using a custom designed network of hybrid couplers to derive the 120 V signal. The modulator crystal is mounted in a balanced stripline transmission line. The modulator driver has an efficiency near 40% and a one nanosecond rise time. The driver has dimensions 22.9 x 15.2 x 8.9 cm (9 x 6 x 3.5 inches).

One of the characteristics of coupling modulation which has not been mentioned up to this point is its frequency response. Its high frequency performance is essentially unlimited, but it has a low-frequency roll-off near 1 MHz.[33] Since normal digital data in the NRZ-L format has a high low-frequency content, the data can be distorted if passed through a coupling modulated system. The desired characteristics of the data spectrum would then be a minimum of low-frequency energy, but no expansion of the signal's frequency spectrum. Figure 26 shows the spectrum of normal NRZ-L data, and that of several coding formats which have the first of the two desired characteristics. The Manchester code is rejected because it doubles the required modulator bandwidth. To date our work has involved the use of the Miller code and we have developed Miller coders and decoders at 100, 200, and 300 Mbps which perform exceedingly close to theoretical values.

The separation of the transmit and receive paths is accomplished by polarization. Figure 27 shows the general technique which is employed. Linear polarization from the transmitter passes through a properly oriented wire grid polarizer with low loss and is then converted to circular polarization by a quarter-wave plate. Circular polarization is desirable because it makes the heterodyne reception process insensitive to terminal rotations about the line-of-sight between the terminals. Incoming circularly polarized energy is converted by the quarter-wave plate to linear polarization, but orthogonal to that of the transmitter. It is, therefore, reflected by the wire grid polarizer. The received energy is then reflected by the LO injection mirror and, collinear with the LO laser beam, illuminates the infrared mixer. Frequency isolation of the transmit and receive channels is obtained by operating the transmitter at least 55 GHz away from the receiver, well beyond the frequency response of the mixer.

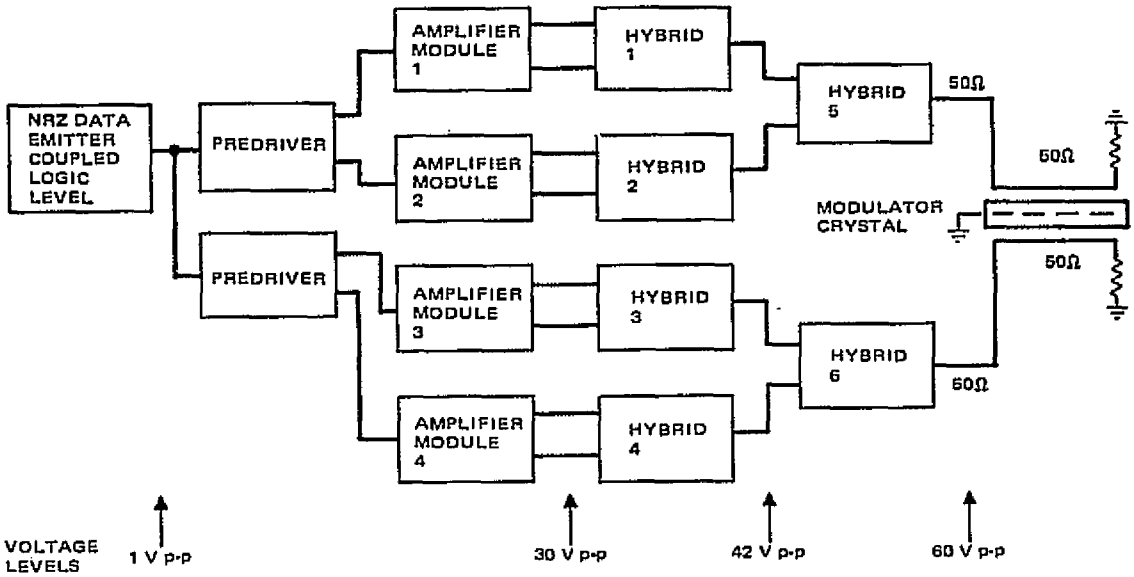

Figure 25. Modulator Driver Block Diagram

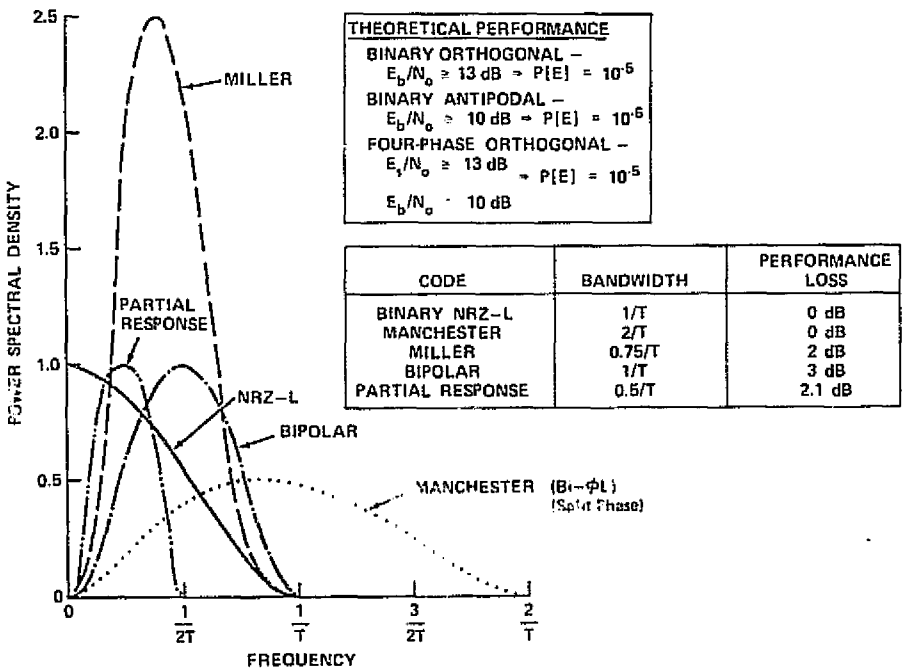

Figure 26. Possible Coding Formats (Refs. 34—38)

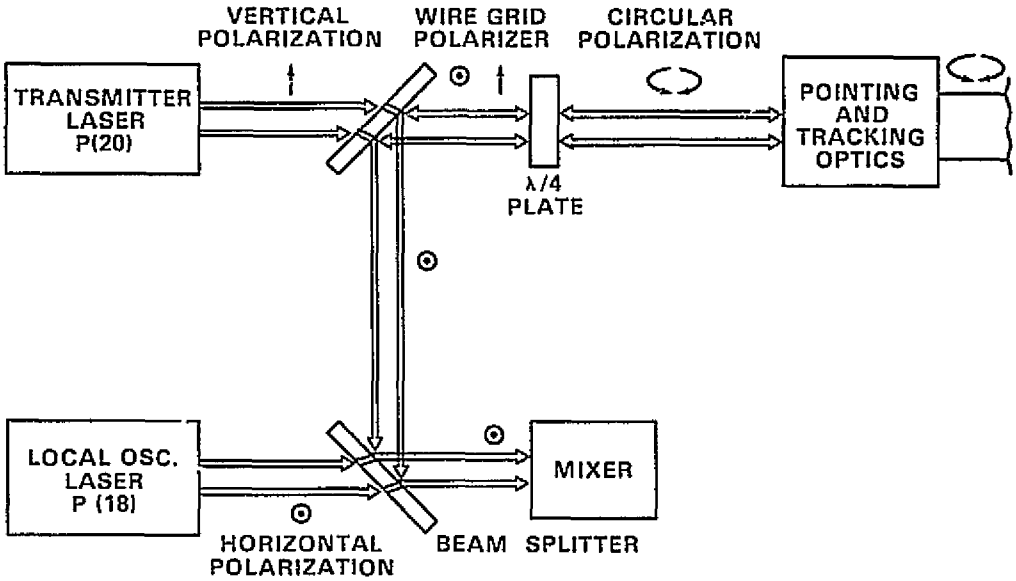

Figure 27. Transmitter-Receiver Optical Diplexing

Laser Lifetime

The lifetime of CO_2 lasers has been a stubborn problem, but is now yielding. With continuing efforts by Goddard Space Flight Center, Hughes, and particularly Hochuli at the University of Maryland, lifetimes beyond 10,000 hours have become routine in conventional CO_2 lasers and similar results are expected in waveguide CO_2 lasers. A sample set of six tubes is now on test to verify the results obtained on a single laser which surpassed 20,000 hours. Of these the eldest has passed 7000 hours and all are continuing on test with satisfactory performance.

CONCLUSIONS

In this paper we have described a five-year program which has produced a receiver engineering model suitable for application in the SRS end of a LAS-SRS data relay link and a transceiver which demonstrates the technology needed in the wideband transmitter subsystem for the LAS. The transceiver also demonstrates the technology required for SRS-SRS data relay. An effort presently underway will produce the hemispherical coverage optical tracking system which is also required by the LAS. That tracking system will be available in mid-1976. We believe that this program has advanced the state-of-the-art to the point that spaceborne CO_2 laser systems have a demonstrated technical feasibility. There are still areas to be improved and certainly any experimental space test of this

technology will have to be meticulously planned and executed. But, in comparison to the 1970 state-of-the-art which led to the initiation of this program,[39] much has been accomplished. Areas which deserve further, although comparatively modest, effort are the improvement of the modulator driver's efficiency and reliability and, of course, the long term demonstration of laser lifetimes commensurate with operational applications, namely 50,000 hours. The system baseline has now been established and future improvements can be measured against that baseline. The first space test of that baseline system has not been identified, but we are confident that such a test will occur and that it will validate the concepts and technology we have described here.

ACKNOWLEDGMENTS

Five year programs of the type described in this paper involve numerous people and, when a paper attempts to sum up such a program, injustice is almost inevitable. We are obviously very grateful to all of the present and former technical contributors from NASA, Hughes, AIL, Arthur D. Little, GTE-Sylvania, S.A.T., the University of Maryland, and the Technical University of Vienna, Austria who made this program succeed. We are also grateful to the individuals who had the often thankless job of supplying the resources for the program. In NASA's Office of Aeronautics and Space Technology, Dr. P. Kurzhals, Mr. C. Pontious, Mr. C. Catoe, and Mr. H. Anderton (now retired) have been staunch supporters, while Mr. E. Ehrlich, Mr. J. Lehmann, Dr. R. Marsten, and Dr. A. Andrus (now retired) in the Office of Applications have provided vigorous and indispensable support.

REFERENCES

1. Operations Research Inc., "Data Origination and Flow for Advanced Earth-Sensing Satellites in 1985 and Beyond," Final Report Contract NAS 5-24034, June 1975.

2. Oliver, B. M. "Thermal and Quantum Noise," Proc. IEEE, Vol. 53, No. 5, May 1965, pp. 436-454.

3. Silver, S., "Aperture Illumination and Antenna Patterns," p. 178 in S. Silver (ed.), Microwave Antenna Theory and Design, McGraw-Hill: New York (1949).

4. Klein, B. J. and Degnan, J. J., "Optical Antenna Gain 1: Transmitting Antennas," Applied Optics, Vol. 13, No. 9, Sept. 1974, pp. 2134-2141.

5. Degnan, J. J. and Klein, B. J., "Optical Antenna Gain 2: Receiving Antennas," Applied Optics, Vol. 13, No. 10, Oct. 1974, pp. 2397-2401.

6. Cohen, S. C., "Heterodyne Detection: "Phase Front Alignment, Beam Spot Size, and Detector Uniformity," Applied Optics, to be published.

7. Peyton, B., DiNardo, A., Kanishak, G., Lange, R., and Arams, F., "High Sensitivity Receiver for Infrared Laser Communications," IEEE J. Quantum Electron., Vol. QE-8, No. 2, Feb. 1972, pp. 246-252.

8. Flattau, T., Mellars, J., "Wideband Infrared Receiver Back-End," Final Report Contract NAS 5-23183, April 1974.

9. Hughes Aircraft Co., "Servo System," Final Report Contract NAS 5-21859, March 1975.

10. Nash, F. R., Smith P. W., "Broadband Optical Coupling Modulation," IEEE J. Quantum Electron., Vol. QE-4, No. 1, Jan. 1968, p. 26.

11. McAvoy, N., Osmundson, J., Schiffner, G., "Broadband CO_2 Laser Coupling Modulation," Applied Optics, Vol. 11, No. 2, Feb. 1972, p. 473.

12. Kiefer, J. E., Nussmeier, T. A., Goodwin, F. E., "Intracavity CdTe Modulators for CO_2 Lasers," IEEE J. Quantum Electron., Vol. QE-8, No. 2, Feb. 1972, pp. 173-179.

13. Hall, D. R., Peruso, C. J., Johnson, E. H., Schiffner, G., McElroy, J., McAvoy, N., "Multichannel Television Coupling Modulation Experiments Using a CO_2 Laser," J. Soc. Photo-Optical Inst. Engr., Vol. 11, No. 3, May 1972, pp. 77-82.

14. Degnan, J. J., "Minimization of the Prime Power Consumption of a Coupling-Modulated Gas Laser Transmitter," Applied Optics, Vol. 13, No. 11, Nov. 1974, pp. 2489-2498.

15. Hughes Aircraft Co., "Design Report Ten Micrometer Wavelength Transmitter," Contract NAS5-20623, 9 May 1975.

16. Wozencraft, J. M., Jacobs, I. M., Principles of Communication Engineering, Wiley: New York (1965).

17. Van Trees, H. L., Detection, Estimation, and Modulation Theory, Part I, Wiley: New York (1968).

18. Forster, D. C., Goodwin, F. E., Bridges, W. B., "Wideband Laser Communications in Space," IEEE J. Quantum Electron., Vol. QE-8, No. 2, Feb. 1972, pp. 263-272.

19. Ross, M., Laser Receivers, Wiley: New York (1966), p. 118.

20. GTE-Sylvania Labs., "Design, Fabrication, Testing, and Delivery of Improved Beam Steering Devices," Final Report Contract NAS8-26846, April 1973.

21. Brewer, S. H., Nussmeier, T. A., "Optical Analysis for Laser Heterodyne Communication System," Final Report Contract NAS5-21898, March 1974.

22. Abrams, R. L., Bridges, W. B., "Characteristics of Sealed-Off Waveguide CO_2 Lasers," IEEE J. Quantum Electron., Vol. QE-9, No. 9, Sept. 1973, pp. 940-946.

23. Nussmeier, T. A., Abrams, R. L., "Stark Cell Stabilization of CO_2 Laser," Appl. Phys. Ltrs., Vol. 25, No. 10, Nov. 1974, pp. 615-617.

24. McElroy, J. H., Thompson, P. E., Walker, H. E., Johnson, E. H., Radecki, D. J., Reynolds, R. S., "Laser Tuners Using Circular Piezoelectric Benders," Applied Optics, Vol. 14, No. 6, June 1975, pp. 1297-1302.

25. Degnan, J. J., "Waveguide Laser Mode Patterns in the Near and Far Field," Applied Optics, Vol. 12, No. 5, May 1973, pp. 1026-1030.

26. Degnan, J. J., Hall, D. R., "Finite Aperture Waveguide Laser Resonators," IEEE J. Quantum Electron., Vol. QE-9, No. 9, Sept. 1973, pp. 901-910.

27. Degnan, J. J., "A Phenomenological Approach to the Design of Highly Tunable Pressure Broadened Gas Lasers," J. Appl. Phys., Vol. 45, No. 1, Jan. 1974, pp. 257-262.

28. Peyton, B. J., "Wideband Infrared Heterodyne Receiver Front-End," Final Report Contract NAS5-23119, August 1974.

29. Cohen, S. C., "Photodiodes for Ten-Micrometer Laser Communications Systems," NASA TM X-524-72-408, Goddard Space Flight Center, Oct. 1972.

30. Arthur D. Little, Inc., "Radiation Cooler for Ten Micrometer Wavelength Engineering Model Receiver," Final Report Contract NAS5-20087, May 1975.

31. McElroy, J. H., "Infrared Heterodyne Solar Radiometry," Applied Optics, Vol. 11, No. 7, July 1972, pp. 1619-1622.

32. Peyton, B. J., Flattau, T., Wolczok, J., Mellars, J., Lange, R. A. "Wideband Heterodyne Receiver for CO_2 Laser Communication Link," Paper 19.9, 1975 IEEE/OSA Conference on Laser Engineering and Applications, May 28-30, 1975.

33. Yariv, A., Nussmeier, T. A., Kiefer, J. E., "Frequency Response of Intra-Cavity Laser Coupling Modulation," IEEE J. Quantum Electron., Vol. QE-9, No. 4, April 1973, p. 594.

34. Lindsey, W. C., Simon, M. K., Telecommunication System Engineering, Prentice-Hall: Englewood Cliffs (1973), pp. 20-22.

35. Hecht, M., Guida, A., "Delay Modulation," Proc. IEEE, Vol. 57, No. 7, July 1969, pp. 1314-1316.

36. Bell Telephone Labs., Transmission Systems for Communications, Bell: Winston Salem (1971), p. 668.

37. Lucky, R. W., Salz, J., Weldon, E. J. Jr., Principles of Data Communication, McGraw-Hill: New York (1968), p. 91.

38. Kretzmer, E. R., "Generalization of a Technique for Binary Data Communication," IEEE Trans. Comm. Tech., Vol. Com-14, No. 2, Feb. 1966, pp. 67-68.

39. McElroy, J. H., "Carbon Dioxide Laser Systems for Space Communications," Proc. Int. Conf. Comm. (ICC'70), Vol. 1, pp. 22-27 to 22-37, 8-10 June 1970.